

Design of a Ku-Band High-Gain Multilayer Corner-Coupled Planar Antenna for Low Earth Orbit Satellite Communications

By William Yates
Student number: 1503280



Faculty of Science and Health
School of Computer Science and Electronic Engineering

Submitted in partial fulfilment of the requirements for the
Degree of Bachelor of Engineering in Electronic Engineering.

Supervisor Professor Dariush Mirshekar-Syahkal

Second Assessor Dr. Amit Singh

April, 2020

Acknowledgements

Firstly, I would like to thank Professor Dariush Mirshekar-Syahkal for his countless hours of support, without his expertise this project would not have been possible and the results would not have been as successful.

I am also thankful to Dr. Amit Singh for his advice on project management and planning.

Finally, I would like to thank my mother and my friends Ivan, Kacper and Jordan for their continuous support and encouragement whilst I was writing this report.

Abstract

This paper looks to investigate methods of obtaining high gain and directivity from a multilayer planar antenna for Low Earth Orbit Satellite communications within the K_u band. Firstly, the issue of internet connectivity in less developed countries is addressed, so a smaller, easier to install antenna is proposed for satellite communication in replacement of a parabolic dish. A simulated 10 dB bandwidth of 500 MHz and directivity up to 13.3 dBi is demonstrated through the vertically-stacked structure with two parasitic directive layers. In conclusion, a link budget shows the featured antenna improves link performance when compared to single-layer patch, and is viable for use in a mobile terminal in place of a parabolic dish.

Contents

List of Figures	v
List of Tables	vii
List of Symbols	viii
1 Introduction	1
2 Literature Review	3
2.1 Project Motivation	3
2.2 Antenna survey	4
2.3 Feeding Techniques	14
2.4 Literature Review Summary	16
3 Design	18
3.1 Initial Design	18
3.2 Second Layer Design	22
3.3 Third Layer Design	26
3.4 Antenna Tuning	29
4 Fabrication	33
4.1 PCB Layout Design	33
4.2 Antenna Construction	34
5 Project Planning	36
5.1 Agile Project Management	36
5.2 Kanban	37
5.3 Development Challenges	37
6 Conclusions	41
6.1 Results	41
6.2 Link Budget Example	45
6.3 Project conclusion	47

List of Figures

2.1	Microstrip antenna layout [1].	9
2.2	Shapes of microstrip antenna elements [1].	9
2.3	Side view of microstrip antenna with fringing electric fields.	10
2.4	The focusing property of a parabolic reflector.	11
2.5	The proposed antenna.	12
2.6	Layers of the antenna [17].	14
2.7	The fully assembled antenna [17].	14
2.8	Diagram of the proposed vertically stacked antenna.	17
3.1	Schematic of the SMA connector [20].	18
3.2	The SMA connector shown in CST Studio Suite®.	19
3.3	The first layer patch.	21
3.4	The S-parameters of the first layer.	21
3.5	The first layer Smith chart	22
3.6	The first and second layer dimensions.	22
3.7	S-parameters for the second layer simulation.	23
3.8	Second layer S-parameters with spacing	24
3.9	E- and H- plane layouts of microstrip patch antennas.	24
3.10	Calculated and measured mutual coupling between two coax-fed microstrip antennas, for both E-plane and H-plane coupling ($W = 10.57\text{cm}$, $L = 6.55\text{cm}$, $h = 0.1588\text{ cm}$, $\epsilon_r = 2.55$, $f_r = 1.4\text{ GHz}$). (Source: D.M. Pozar, "Input Impedance and Mutual Coupling of Rectangular Microstrip Antennas," <i>IEEE Trans. Antenna Propagat.</i> , Vol. AP-30, No. 6, November 1982. ©1982 IEEE).	25
3.11	The second and first layer model.	26
3.12	First simulation for third layer where $h = 5\text{mm}$	26
3.13	Smith chart showing mismatched input impedance	27
3.14	Comparing Smith chart plots with respect to third layer substrate thickness.	27
3.15	The three layer stacked patch antenna with the foam height at 8mm.	28
3.16	Directivity and S-Parameters for a third layer height of 8mm.	29
3.17	Analytical line impedance of the co-axial probe.	30
3.18	Foam height parameter sweep from 5mm to 12mm.	30

3.19	Smith chart showing 50Ω impedance matching at 11.95 GHz.	31
3.20	The S-parameters for the final design.	32
3.21	VSWR for the final design.	32
3.22	The final design layout.	32
4.1	First and second layers of the antenna on Duroid [®] 5880 substrate.	33
4.2	First and second layers of the antenna on Duroid [®] 5880 substrate.	34
4.3	Third layer fastened with nylon screws.	35
4.4	Side view of the antenna.	35
5.1	Agile development block diagrams.	36
5.2	Kanban workflow.	37
5.3	Cumulative flow diagram from kanban board	38
5.4	This figure shows a risk being reported and the entire kanban board.	40
6.1	Antenna directivity from 12.3 - 13.3dBi.	42
6.2	E-phi radiation pattern at 11.95 GHz where phi = 0.	43
6.3	Absolute radiation pattern at 11.95 GHz	44
6.4	Absolute linear directivity at 11.95 GHz	44
6.5	BER as a function of SNR.	45

List of Tables

2.1	Antenna Dimensions.	13
2.2	Comparison of feeding methods.	16
2.3	Antenna specification.	17
3.1	Antenna dimensions.	22
3.2	Initial dimensions for second layer.	23
3.3	Optimised dimensions for second layer.	23
3.4	Second layer S-parameters and directivity with different spacing lengths. . . .	23
3.5	Patch dimensions after first acceptable simulation.	28
6.1	Table of the final antenna dimensions.	41
6.2	Operating parameters for the final design.	43
6.3	Ground station parameters.	46
6.4	Downlink station parameters.	46
6.5	CNR comparison for 7.5dBi and 12.8dBi receiver antennas.	46

List of Symbols

λ_0	Free Space Wavelength
ϵ_r	Relative permittivity
v_0	Free-space Velocity of Light
ADS	Advanced Design System
B	Channel bandwidth
BER	Bit Error Rate
BW	Bandwidth
c	Speed of Light in vacuum
CNR	Channel-to-noise ratio
dB	Decibel
dB _i	dB (isotropic)
E _b	Energy per bit
EIRP	Effectve Isotropically Radiated Power
f _b	Channel data rate
HTS	High Throughput Satellite
ITU	International Telecommunication Union
K _a	Kurz-above
K _u	Kurz-under
LEO	Low Earth Orbit
LHC	Left Hand Circular
N ₀	Noise Power

ODU	Outdoor Unit
PCB	Printed Circuit Board
PFD	Power Flux Density
Q	Quality Factor
RHC	Right Hand Circular
SMA	SubMiniature version A
SNR	Signal-to-noise ratio
VSAT	Very Small Aperture Terminal
VSWR	Voltage Standing Wave Ratio
W	Watts

Chapter 1

Introduction

Microstrip or patch antennas are frequently used when operating in the K_u band and have numerous design advantages. They are low profile, conformable to planar and non-planar surfaces, simple to manufacture, mechanically robust, and easily adaptable in terms of resonant frequency, impedance, radiation pattern and polarisation [1]. Given the advantages, microstrip antennas are a suitable candidate as a part of a LEO satellite receiver terminal.

The significant operational disadvantages of microstrip antennas are their low efficiency, low power, high Q-factor (Q) and narrow frequency bandwidth (BW). Alongside the disadvantages, the typical gain of a patch antenna is generally low. The gain of an antenna is inversely proportional to its beamwidth, meaning a narrower beam results in increased power, transmitted or received, this means smaller user terminals can be used. In the case of a satellite downlink terminal, improving receiver gain enhances the Carrier-to-noise-ratio (CNR) of the system and allows for the use of higher order modulations, resulting in a higher rate of data transmission and reduced Bit-error-rate (BER) [2].

The purpose of this project is to improve the gain of a planar microstrip antenna within a portable satellite communication terminal. The proposed configuration involves a stacked microstrip antenna consisting of a coaxially fed patch that drives four electromagnetically coupled patches. A third layer made up of four patches is then introduced to achieve a high gain of about 13dBi. In patch arrays, the feed network losses degrade performance in sidelobes, cross polarisation, gain and noise temperature [3]. In the layout mentioned, the four patches are not physically connected in an effort to eliminate feed network losses.

This report is divided into 6 chapters. The literature review outlines the aims of the project and explains how they can be achieved. After the context has been provided, the project aims and objectives are outlined. All technical documentation related to the project has

been uploaded to a GitLab repository and will be referenced during the report [24]. The design chapter covers the initial design calculations and simulations, rounded up by antenna tuning. A look at the fabrication method showcases the final product. Project planning is discussed, explaining the development methodologies and risk management methods used. Finally, a concluding chapter reviews the outcomes of the project and a clear distinction between design goals and end product is made. An example link budget showcases the antenna's viability in a VSAT when compared with another antenna. Suggestions for future work and improvements are also considered.

Chapter 2

Literature Review

2.1 Project Motivation

Connectivity is a key part of modern society and the Internet has become an important utility for a majority of the world. The Internet is gradually replacing the home telephone and television as it becomes a hub for communication, information and entertainment, as a result more people require access [6]. According to research produced by the University of Washington, it is important for people to have access to the Internet because it connects them to the information and skills needed in an increasingly digital world [10].

An estimated 4.1 billion people were using the Internet in 2019 with 87% of these coming from developed countries [7]. Although the Internet is crucial to the modern world, 3.6 billion people remain unconnected, despite 97% of the global population being within range of a mobile signal, and 93% of the global population being able to access 3G or higher mobile broadband services [7]. A majority of the population who are unconnected reside in less developed countries where barriers to connectivity include affordability and low income, infrastructure, user capability and illiteracy. Internet connection can facilitate vital services operating in unconnected regions and help the development of key sectors such as education, healthcare, government and farming [9]. The infrastructure needed to connect 1.5 billion unconnected people has been estimated to cost \$450 billion, making it very expensive for less developed countries to gain access to the Internet. In countries and communities that cannot afford to invest in expensive fronthaul or backhaul networks, VSATs offer an affordable solution to Internet connectivity.

A VSAT can be a one-way or two-way satellite ground station that can access satellites in a variety of orbits, including Geostationary, Elliptical or Low Earth Orbit. A one-way network involves a hub transmitting carriers to receive-only terminals, this is commonly used

in broadcasting. A two-way network allows a VSAT to transmit and receive, this supports broadband connectivity. VSATs are often installed with parabolic dish antennas but, due to cheaper fabrication and installation costs, microstrip arrays are also used. The production and installation costs of antennas can be prohibitively high for less developed countries, and hence, the people who would benefit from VSATs the most. Thus, this paper seeks to investigate the design, simulation, and fabrication of a lower cost, high-gain microstrip antenna.

2.2 Antenna survey

Antennas are the fundamental components of any wireless communication system that allow signals from a wired system to be transferred to electromagnetic waves. The receiving and transmitting functionality of an antenna is outlined by James Clerk Maxwell's equations [3]. The purpose of the antenna survey is to analyse, compare and evaluate antennas that could be used as a part of a VSAT.

This project will be concerned with the development of a receive antenna with the idea that a similarly designed transmitting aperture may coexist in the same terminal operating at a different frequency. The receive antenna must meet the following design criteria:

- *Frequency band.* Satellite networks operate in a number frequency bands such as C, X, K_u and K_a. For this project, the K_u band has been chosen, where the operating frequency should lie between 11.7 to 12.2 GHz to comply with the receiving frequency in a 11/14 GHz downlink/uplink system.
- *Size.* The antenna must be smaller than the majority of current VSAT terminal antennas, that is less than 75cm x 75cm x 10cm. The smaller the antenna, the easier and more cost effective the Outdoor Unit (ODU) is to install.
- *Lightweight.* The antenna should weigh less than similar devices in the K_u band.

2.2.1 Antenna Parameters

There are numerous parameters that characterise the performance of antennas, for this project the most significant characteristics are reviewed. These are:

- *Reflection coefficient and voltage standing wave ratio.* This is a coefficient and ratio of power radiated by the antenna.
- *Input impedance.* A measure of opposition to current at the input of the antenna.
- *Polarisation.* This is the geometric orientation of the electromagnetic waves propagated by the antenna.
- *Directivity.* Concentration of radiation emitted by the antenna in a single direction.
- *Bandwidth and Quality factor.* Range of frequencies that antenna radiates and the ratio of centre frequency to bandwidth.
- *Antenna efficiency.* This is a ratio of the power delivered to an antenna relative to the power radiated.

2.2.1.1 Reflection Coefficient and Voltage Standing Wave Ratio

For a single-port antenna, the scattering parameters (S-parameters), S_{ii} , describe the input-output relationship between ports. S_{ii} relates the outgoing wave voltage at port i , V_i^- with the incoming wave voltage, V_i^+ [13].

$$\Gamma_i \equiv \frac{V_i^-}{V_i^+} \quad (1)$$

The reflection coefficient, Γ_i is equal to the scattering coefficient, S_{ii} in a single-port antenna. If the magnitude is less than or equal to 1, the antenna is said to be passive.

The Voltage Standing Wave Ratio (VSWR) is ratio of the maximum and minimum voltages on the transmission line connected to the antenna and is related to the reflection coefficient, Γ as

$$VSWR = \frac{1 + |\Gamma|}{1 - |\Gamma|} \quad (2)$$

S-parameters are an important representation of antenna behaviour with regards to the circuit the antenna is connected to because they display how much power is being radiated by the antenna and how much is being reflected. When an antenna is not matched to the receiver,

power is reflected, that is, $\Gamma \neq 0$. This results in a reflected "voltage wave" that causes standing waves along the transmission line. When the VSWR = 1, there is no reflected power and the voltage maintains a constant magnitude along the transmission line.

In the field, antennas are analysed on a pass/fail criteria based on VSWR specifications. For this project the acceptable centre frequency VSWR is 1.5 (14dB) with 1.92 (10dB) for the sidebands. For this report, return loss will primarily be conveyed through S-parameters

2.2.1.2 Input Impedance

Input impedance of an antenna, Z_A , is the ratio of voltage V and current I at the input of the antenna. The input impedance may be determined from the reflection coefficient, Γ and the characteristic impedance Z_C of the transmission line connected to the input of the antenna; that is,

$$Z_A \equiv \frac{V}{I} = Z_C \frac{1 + \Gamma}{1 - \Gamma} \quad (2.1)$$

which means,

$$\Gamma = \frac{Z_A - Z_C}{Z_A + Z_C} \quad (2.2)$$

By matching the line impedance and antenna impedance, maximum power transfer may be achieved. There are two equations that may be used to approximate the edge impedance of a patch of the antenna.

$$Z_A = \begin{cases} \frac{120\pi\sqrt{\epsilon_{\text{eff}}}}{\frac{W}{h} + 1.393 + 0.667\ln(\frac{W}{h} + 1.444)}, & \text{for } \frac{W}{h} \geq 1 \\ \frac{60}{\sqrt{\epsilon_{\text{eff}}}} \ln \left(\frac{8h}{W} + 0.25 \frac{W}{h} \right), & \text{for } \frac{W}{h} \leq 1 \end{cases} \quad (2.3)$$

The variables involved shall be discussed later, what is important is knowing how to approximate the antenna's impedance, allowing an estimation of the reflection coefficient to be made.

Impedance is also be represented as a complex number in the form $Z = R + j\Omega$. The real part, R , represents the power radiated or absorbed by the antenna. The imaginary part, j , signifies power stored in the near field of the antenna, this is also referred to as non-radiated power. It is important that the imaginary part remains at zero so the antenna becomes a resonant structure.

2.2.1.3 Polarisation

The polarisation of an antenna in a specified direction is the polarisation of the plane wave transmitted or received by the antenna. For plane waves, the polarisation properties of the electric field vector are specified because the magnetic field vector is simply related to the electric field vector. The polarisation field comprises of the electric and magnetic fields and is orthogonal to the direction of propagation. It is important to match the polarisation of an antenna to that of an incoming signal to ensure the strong signal clarity. If there is a mismatch of antenna polarisation, there is a corresponding decrease in signal level.

There are several categories of polarisation:

- *Linear Polarisation.* Linear polarisation characterise radiation that propagates in one plane. According to Zürcher and Gardiol (1996), basic patch antennas with rectangular shape have linear polarisation [15].
- *Circular Polarisation.* Circular polarisation is a state where, at each point, the electromagnetic field of the wave has constant magnitude. The wave's direction rotates at a constant rate perpendicular to the direction of the wave.
 - *RHC.* The polarisation vector rotates in a right-handed sense with respect to the direction of propagation.
 - *LHC.* The polarisation vector rotates in a left-handed sense with respect to the direction of propagation.
- *Elliptical Polarisation.* Similar to circular polarisation where the tip of the electric field vector outlines an ellipse.

2.2.1.4 Directivity

According to the 1983 version of the *IEEE Standard Definitions of Terms for Antennas*, the directivity of an antenna D is; "The ratio of the radiation intensity in a given direction from the antenna to the radiation intensity averaged over all directions. The average radiation intensity is equal to the total power radiated by the antenna divided by 4π . If the direction is not specified, the direction of maximum radiation intensity is implied."

$$D = \frac{U}{U_0} = \frac{4\pi U}{P_{\text{rad}}} \quad (2.4)$$

Where U (W/unit solid angle) represents radiation intensity , U_o (W/unit solid angle) is the radiation intensity of an isotropic source and P_{rad} is total radiated power (W).

Antenna directivity is measured in dB (isotropic), dBi, this is the gain of an antenna compared to the gain of an isotropic antenna. An isotropic antenna is an ideal source that radiates power uniformly in all directions.

2.2.1.5 Bandwidth and Quality Factor

Antenna bandwidth describes the range of frequencies which the antenna can radiate energy, this is usually subject to meeting certain specifications. The bandwidth of an antenna could be the range of frequencies either side of the centre frequency up to a certain threshold. Q is the ratio of an antenna's centre frequency to its bandwidth. Q is inversely proportional to bandwidth so that $Q = \frac{1}{BW}$, a high Q results in a narrowband antenna and low Q means the antenna is wideband.

2.2.1.6 Antenna Efficiency

Antenna efficiency is the ratio of power received to the power radiated from the antenna. A high efficiency antenna radiates a majority of the energy it receives. A low efficiency antenna absorbs or reflects a majority of the power received. Efficiency can therefore be represented as $e = \frac{P_{radiated}}{P_{input}}$. Antenna efficiency may often be represented as a percentage or in dB, for example, $e = 0.5 \equiv 50\% \equiv -3dB$.

2.2.2 Microstrip Antenna

The first practical microstrip antenna was constructed by J.Q. Howell in 1972 [4]. The simplest microstrip antenna is a radiating patch of metal on top of a dielectric substrate, mounted over a ground plane. There are many substrates that can be used for the design of patch antennas, with their dielectric constants usually in the range of $2.2 \leq \epsilon_r \leq 12$. For desirable antenna performance, a thick substrate with a low dielectric constant will provide better efficiency and have larger bandwidth, at the expense of a slightly bigger structure [1].

The radiating elements can be square, rectangular, circular or any other two-dimensional shape Figure 2.1 shows a square patch configuration. Figure 2.2 illustrates some common shapes used in microstrip antennas. Square, rectangular, dipole and circular are commonly used because they are simple to fabricate and analyse. A major advantage of a microstrip antenna is its small size and light weight, this is why they are used in modern satellite communication systems, both on the spacecraft and other applications that require portability.

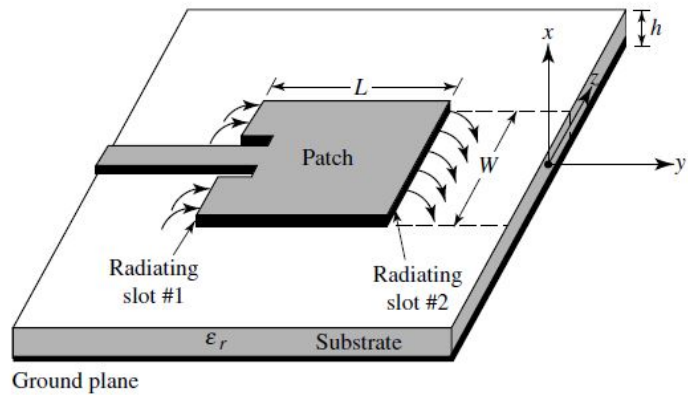


Figure 2.1 – Microstrip antenna layout [1].

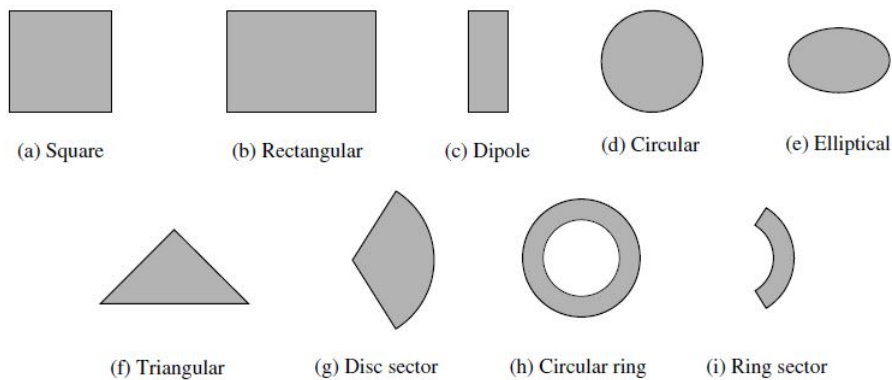


Figure 2.2 – Shapes of microstrip antenna elements [1].

The fringing fields around a microstrip antenna explain why patch antennas radiate. Looking at Figure 2.3, current at the edge of the patch is zero, and represents an open circuit. The current has the highest value at the centre of the (half-wave) patch and is, in theory, zero at the edges. The low amount of current at the edge of the patch explains why the impedance is highest at the edge.

Since microstrip patch antennas are viewed as open circuit transmission lines, $\Gamma = 1$. When $\Gamma = 1$, the voltage and current are out of phase, this mean voltage is at a maximum at the end of the patch and minimum at the start. This the electric field underneath the patch will be similar to the one shown below. Fringing fields are the reason why microstrip antennas radiate because they add up in phase alongside the same direction, for this example, this is done in the y-direction. The antenna's radiations arises from the fringing fields because of the

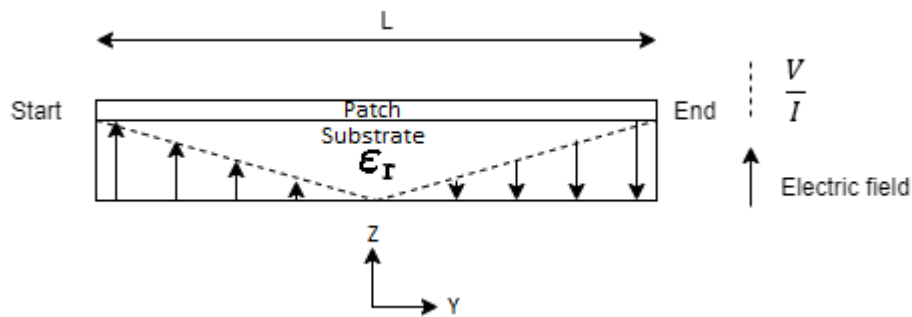


Figure 2.3 – Side view of microstrip antenna with fringing electric fields.

voltage distribution and not the current, hence it is referred to as a "voltage radiator", other than a "current radiator", like a wire antenna.

The advantages of microstrip antennas include:

- *Light weight.* Microstrip patch antennas do not weigh much because they are often made from a thin copper layer usually ($36 \mu\text{m} = 152 \text{ g/m}^2$) or ($17 \mu\text{m} = 305 \text{ g/m}^2$) thick [5].
- *Low cost.* Fabrication involves a cheap printed-circuit technique. The most expensive part of the antenna is usually the dielectric substrate.
- *Low profile.* The thickness of a microstrip patch antenna is normally less than $0.03\lambda_0$.
- *Conformable to planar and non-planar surfaces.* The antenna can be fabricated on a planar or non-planar surface and conform to the dielectric substrate it attaches to.
- *Easy to integrate in circuits.* It is easy to use microstrip patch antennas in arrays or to incorporate them with other microstrip circuit elements.
- *Versatile.* The properties of a microstrip patch antenna can be adjusted to suit different applications. Adaptable properties include impedance, resonant frequency, radiation pattern and polarisation, these properties change by choice of element shape and feeding arrangement. This allows for certain parameters to be modified so that they are best suited for LEO satellite communication.

The disadvantages of microstrip antennas include:

- *Low efficiency.* This is because antenna efficiency is a function of gain and directivity. Since microstrip antennas conventionally have low gain (6 - 9dBi) the efficiency is usually no more than 90%. [30]

- *Low gain.* As mentioned before, a single-patch microstrip antenna normally has a gain of 6 - 9dBi, in contrast a parabolic reflector may reach a gain of 20dBi or more [31]. The low gain is due to the small effective area of the antenna.
- *Narrow frequency bandwidth.* This is due to the inverse relationship with the Q factor. Having a large bandwidth is important because it allows for higher data rates to be achieved in a communications channel [28].

2.2.3 Parabolic Reflector

Parabolic reflectors are commonly used for satellite communications to enhance the gain of antennas for point-to-point communications [29]. The basic structure of a parabolic reflector antenna is a curved surface with a cross-sectional shape of a parabola. The reflector provides a focusing mechanism that concentrates energy in a clear direction.

The main property of the reflector is the focusing, where parallel electromagnetic waves making contact with the reflector converge on a single point, known as the focus. Conversely, waves originating at the focus are reflected in the form of a parallel beam along the axis of the reflector. Figure 2.4 illustrates this, where F is the focus.

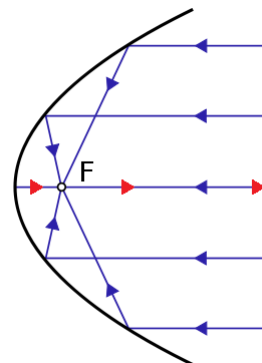


Figure 2.4 – The focusing property of a parabolic reflector.

The blue arrows represent incoming waves and the red arrows represent the reflected plane wave.

2.2.4 High Gain Patch Antennas

2.2.4.1 A New Stacked Microstrip Antenna With Large Bandwidth And High Gain

In 1993 H.Legay and L.Shafai presented a stacked microstrip antenna with high gain and bandwidth [16]. It consisted of four identical patches uniformly laid out within a rectangular

aperture, and electromagnetically fed by a driven patch on a lower substrate. The antenna is shown in Figure 2.5.

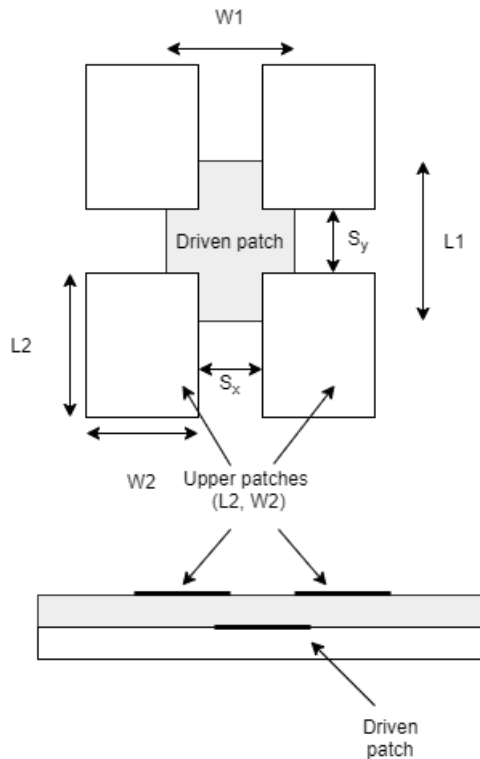


Figure 2.5 –The proposed antenna.

Legay and Shafai explain that according to transmission line theory, the open circuits realised by the radiation edges of the driven patch are located underneath the upper patches. This attracts the fringing fields, allowing for a strong electromagnetic coupling along with the potential for large bandwidth. According to the paper, a narrow spacing between the upper patches moves the radiating edges of the lower patch closer to the transverse axis of the upper patches and as a result, increases coupling. Strong coupling is required because poor coupling will adversely affect parameters like the reflection coefficient and impedance; these parameters have great influence on radiation characteristics and their deterioration will severely impact the performance of the antenna. Although the level of coupling between the lower patch and a single upper patch is minor, the combined coupling levels for all four patches allows the antenna to get to the critical coupling coefficient required for the input impedance.

Due to a large number of parameters, the antenna may be designed to optimise specific characteristics, such as bandwidth, gain, directivity and cross polarisation. Increasing

bandwidth will open the opportunity for faster data rates whilst high gain, directivity and polarisation matching will increase the CNR. The spacing between the upper patches is the most sensitive parameter because it affects the coupling and the field distribution within the subarray, as explained previously strong coupling is required for low reflection loss.

Large spacing increases the antenna size and therefore, the directivity, but reduces the coupling size area between the upper and lower patches, affecting the bandwidth. It was shown that the substrate thickness ratios affects coupling. Patch width influences polarisation purity and gain. A key design note with this antenna is that the length of the lower patch must be longer than the upper ones; This is to cancel out the imaginary component of the input impedance.

The added benefit of this configuration is the high gain (12dBi) without an array feed network. In microstrip arrays the feed network may decrease operating performance in antenna gain, cross polarisation and the noise temperature.

2.2.4.2 Yagi-like Microstrip Patch Antenna With High Directivity

When investigating multilayer patch antennas, J. A. Nessel et al achieved high gain and directivity using a similar technique to Legay and Shafai [16] [17]. The antenna structure has two key compartments, the radiator and the parasitic directors which are stacked on top of the patch. The radiator is made up of a driven patch antenna with a reflector on a substrate below which is connected to ground. The substrate used, Duroid[®], has a $\epsilon_r \approx 2.2$. The antenna layers and dimensions are shown below in Table 2.1 and Figure 3.16.

Table 2.1 – Antenna Dimensions.

Dimensions					
Variable	Length (mm)	Variable	Length (mm)	Variable	Length (mm)
h1	0.5	L	10	L _D	8.95
h2	0.13	W	10.05	W _D	9
h3	0.13	d _i	2.73		
W _R	10.55	W _i	15.88		
W _L	10.5	L _F	12.7		
		W _F	0.5		

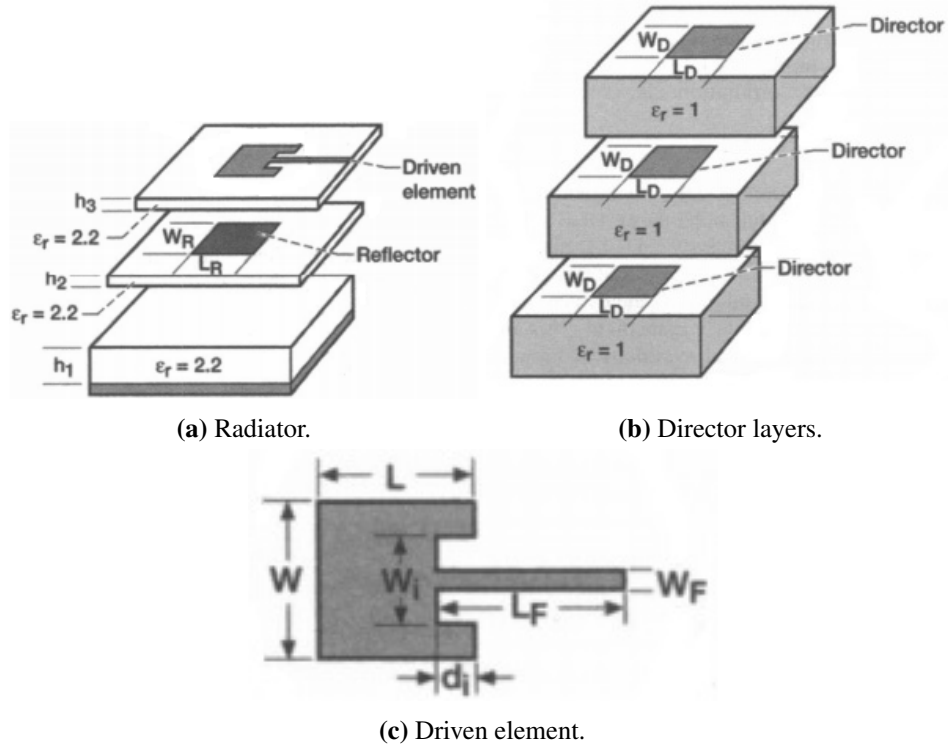


Figure 2.6 – Layers of the antenna [17].

The director microstrip patches are mounted on foam with a $\epsilon_r \approx 1$. The directors' size is approximately $0.8A$, A being the area of the driven patch. The layer spacing between directors is $0.3\lambda_0$. Figure 2.7 shows the completed antenna.

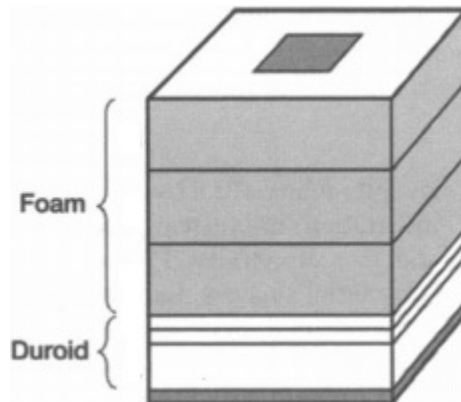


Figure 2.7 – The fully assembled antenna [17].

2.3 Feeding Techniques

An antenna feed is used to excite the radiating element of an antenna directly or indirectly. It is also the place where the feed's impedance is converted to the antenna's intrinsic impedance so they can be matched if needed to.

The feeding method effects the fundamental characteristics and input impedance of the antenna. The four most popular configurations to feed a microstrip are the microstrip line, coaxial probe, aperture coupling and proximity coupling [1].

A microstrip-line feed is easy to model, fabricate and match. Although, as the substrate thickness increases, surface waves and spurious feed radiation increases, which can limit the bandwidth to typically 2-5%.

A coaxial-line feed is non-planar feeding technique, where the inner conductor of the coax is used to feed the radiation patch. The outer conductor of the cable is connected to the ground plane. According to Chakravarthy et al, one of the advantages of using a coaxial feed is the ability to place the coaxial probe anywhere on the patch as a method of impedance matching [11]. For thicker substrates, it is harder to match impedance due to probe inductance and probe radiation. The probe may also generate cross-polarised fields if electrically thick substrates are implemented [11].

Aperture-coupling feeds involve two dielectric substrates, one for the antenna and the other for the feed. A ground plane with a slot in the centre separates the two substrates. At the bottom of the lower substrate there is a microstrip feed line, the energy of which couples to the top layer patch through the ground plane slot. This configuration allows independent optimisation of the feed and radiating element. For this arrangement, the antenna substrate is usually thicker and has a higher dielectric constant than the lower substrate. Impedance matching is performed by controlling the width of the feed line and the length of the slot.

Proximity-coupling, like aperture-coupling, involves two substrates, but there is no slot in the ground plane. Instead, the ground plane lies on the bottom part of the lower substrate. This means the patch is fed through the microstrip line with a layer of dielectric substrate between them. Two layers of substrate can increase the bandwidth with the appropriate positioning. Proximity-coupling has been shown to have the largest bandwidth (as high as 13%) and good radiation performance [1], [11], [12].

The survey carried out by Chakravarthy et al collected and compared results of the feeding methods used to drive an antenna with a resonant frequency of 2 GHz.

Table 2.2 – Comparison of feeding methods.

	Inset feed	Co-axial probe	Proximity coupling	Aperture coupling
Bandwidth (MHz)	42.5	42.1	70	144.1
S-parameters (dB)	-16.11	-20	-18.2	-37.9
Directivity (dBi)	7	5.4	5.6	6.5
Beamwidth (°)	92.4	104.3	101.7	84.9
Side lobe level (dB)	-12.4	-4.9	-6.6	-9.9
VSWR	1.3	1.4	1.3	1.1

2.4 Literature Review Summary

The literature review has provided a background as to how the antenna should perform and the parameters required for it to be useful inside a VSAT. The antenna should be small and lightweight whilst offering high-gain, high directivity and enough bandwidth to support its application. Since the antenna chosen should be low profile, a parabolic reflector would not be suitable because of its size.

The proposed microstrip antenna offers a combination of the ideas from Legay and Shafai, and Nessel et al. The idea is to tune an antenna to a centre frequency of 11.95 GHz via the methods of Legay and Shafai for high gain and bandwidth. A third layer consisting of four tuned patches will be placed on a substrate with $\epsilon_r \approx 1$ to act as a director, as seen in Nessel et al. The expected result is a high gain, high directivity and high bandwidth receive antenna suitable for use in a VSAT.

Although a co-axial probe does not have the best performing S-parameters or directivity, it has the lowest side-lobe levels and is simple to model. The co-axial feeding method was also chosen for easier impedance matching.

The antenna specification based on the literature review and technical documentation is shown below.

Table 2.3 – Antenna specification.

Antenna characteristics	
Parameter	Requirement
Resonant Frequency	11.95 Ghz
Bandwidth	11.7 - 12.2 GHz
Directivity	> 12dBi
Beamwidth	< 60°
Polarisation	Linear, RHCP or LHCP.
Dimensions	< 75cm x 75cm x 10cm
Weight	< 100g
Feeding method	50Ω thin co-axial probe

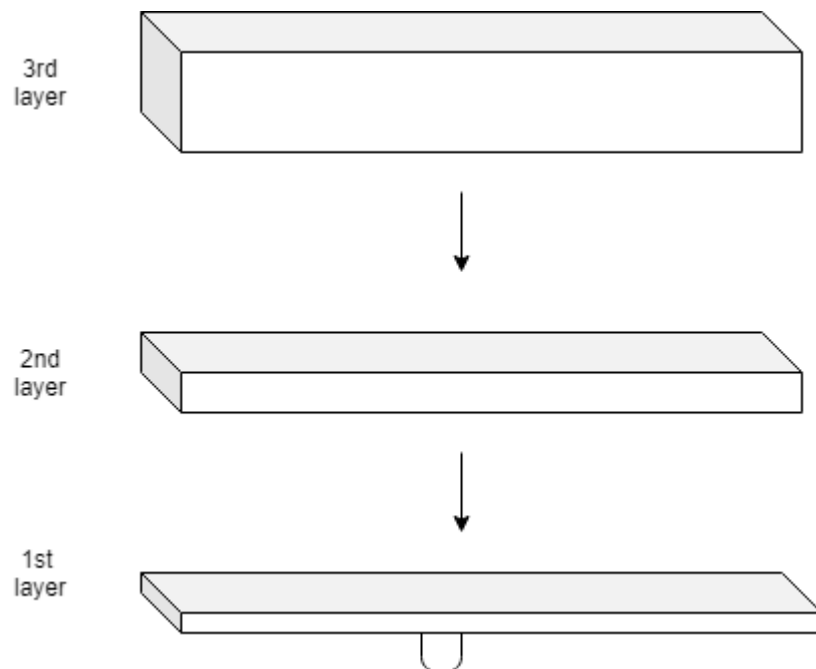


Figure 2.8 – Diagram of the proposed vertically stacked antenna.

Chapter 3

Design

3.1 Initial Design

3.1.1 Feeding Technique

The review of feeding methods seen in S. Chakravarthy et al suggests that coaxial-fed microstrip antennas have high beamwidth with small side lobes [11]. This makes co-axial probe feeding a suitable technique for a high-directivity antenna. A coaxial probe is simple to model once the appropriate connector has been found. For this design, a 50Ω SubMiniature version A (SMA) with a 0.25mm inner-core has been selected with a standard input diameter of 1.3mm, see Figure 3.1.

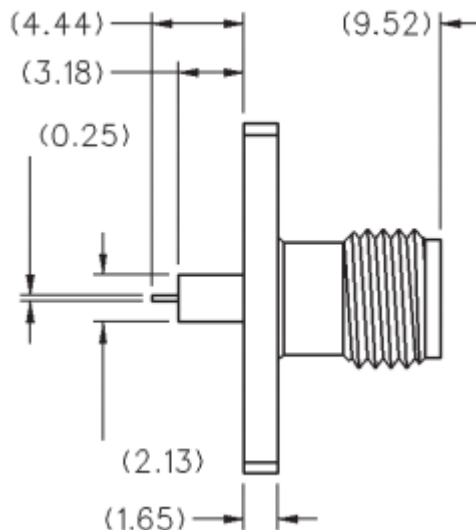


Figure 3.1 – Schematic of the SMA connector [20].

Following the dimensions provided in the connectors' datasheet, the pin was modelled using CST Studio Suite® and is shown below.

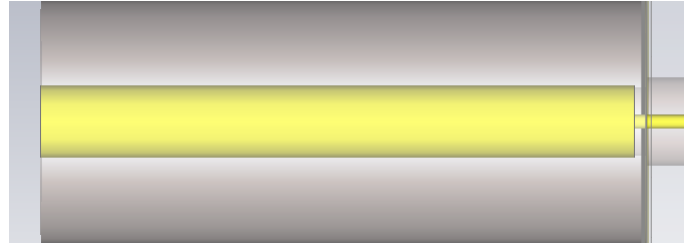


Figure 3.2 – The SMA connector shown in CST Studio Suite®.

3.1.2 Substrates

As stated by L. Shafai, the lower patch requires stronger coupling and must be on a thin dielectric substrate with a thickness of $\leq 0.04\lambda_0$ [18]. For the first two layers of the antenna, Rogers Duroid®5880 has been chosen with a $\epsilon_r = 2.2$. According to Pozar, lower permittivity allows for wider bandwidth and a smaller number of surface waves. Thicker substrates were also shown to have good bandwidth but less coupling [21]. Since $\lambda_0 \approx 1\text{mm}$ at 11.95 GHz, the first layer height was chosen to be 0.78mm, Shafai states that the second layer should be slightly thicker so the next available height of 1.27mm was chosen [18].

The third layer should be placed on a material with a $\epsilon_r \approx 1$. ROHACELL®31HF is a closed-cell rigid foam based on polymethacrylimide chemistry that is designed specifically for antenna applications. ROHACELL®31HF has a $\epsilon_r = 1.046$ and a loss tangent of 0.0017 at 10 GHz. The material thickness is available from 1-120mm. Initially a thickness of $0.3\lambda_0 = 7.5\text{mm}$ was selected [17].

3.1.3 First Layer Design

The design begins with the lower patch on the first layer. According to Shafai, a good starting point for a multi-layer resonant structure is to design the lower patch using the low frequency limit, that is 11.7 GHz [18]. Conventional design equations shall be used to design a first layer with 11.7 GHz as the resonant frequency.[1, ref chapter and page].

To determine the width W and length L of the patch, there are three key parameters that have to be established, ϵ_r , f_r (in Hz) and height h . For the first layer $\epsilon_r = 2.2$, $f_r = 11.7 \times 10^9$ and $h = 0.78\text{mm}$.

The design procedure is as follows:

1. For the radiator, a practical width with good radiation efficiency may be obtained from [19]

$$W = \frac{1}{2f_r\sqrt{\mu_0\epsilon_0}} \sqrt{\frac{2}{\epsilon_r + 1}} = \frac{c}{2f_r} \sqrt{\frac{2}{\epsilon_r + 1}} \quad (3.1)$$

2. Find the effective dielectric constant of the patch antenna, using

$$\epsilon_{\text{eff}} = \frac{\epsilon_r + 1}{2} + \frac{\epsilon_r - 1}{2} \left(1 + 12 \frac{h}{W} \right)^{-1/2} \quad (3.2)$$

because $W/h \geq 1$.

3. Once W has been calculated, the extension length ΔL , can be found

$$\Delta L = 0.412h \frac{(\epsilon_{\text{eff}} + 0.3) \left(\frac{W}{h} + 0.264 \right)}{(\epsilon_{\text{eff}} - 0.258) \left(\frac{W}{h} + 0.8 \right)} \quad (3.3)$$

The effective length is related to the resonant frequency.

$$L_{\text{eff}} = \frac{c}{2f_r\sqrt{\epsilon_{\text{eff}}}} \quad (3.4)$$

4. The physical length of the patch is found using

$$L = L_{\text{eff}} - 2\Delta L \quad (3.5)$$

Using equation 4.2 with the parameters mentioned, an approximate width of 10.13mm was calculated. Equation 4.1 produces a ϵ_{eff} of 2.03. $\Delta L = 0.4\text{mm}$, the effective length = 9mm the actual length, $L \approx 8.2\text{mm}$. To calculate the edge impedance of the patch, equation 2.2 was used and the 50Ω coordinate was found to be 37% horizontally from the edge. Figure 3.3 shows the 3D model of the first layer on 50x50mm of substrate and Figure 3.4 shows the S-parameters. The resonant frequency is 11.7 GHz as expected. Initially, the first layer parameters determined in this section will be used with the second layer.

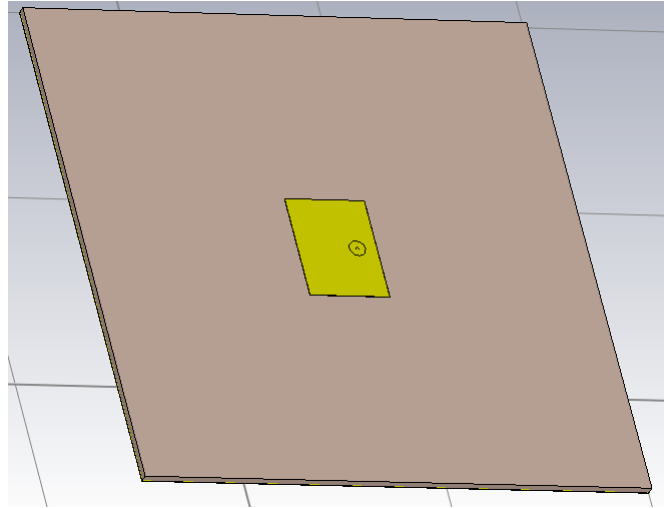


Figure 3.3 – The first layer patch.

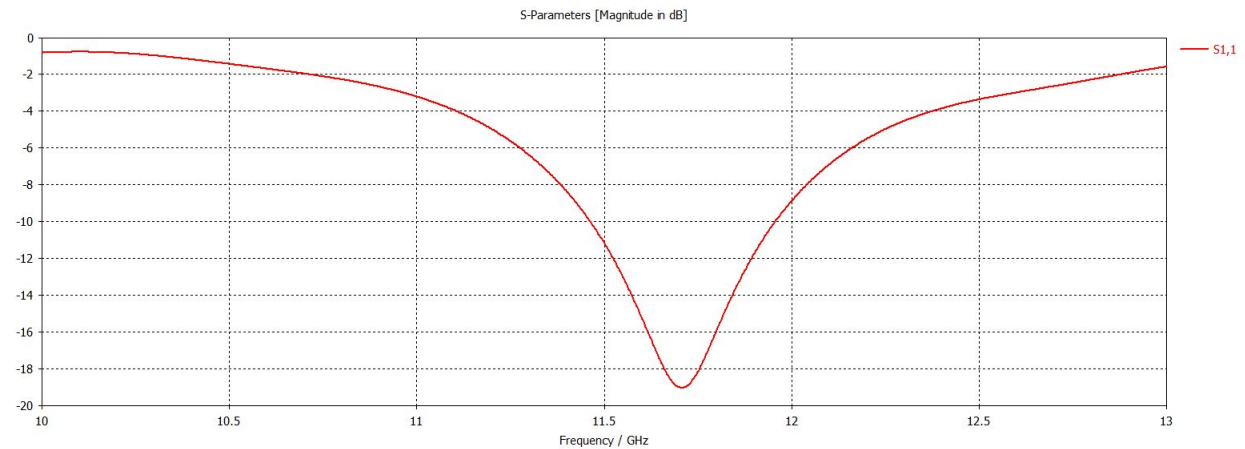


Figure 3.4 – The S-parameters of the first layer.

Although impedance on the Smith chart is not matched 50Ω (Figure 3.5), progression to the second layer design is still to be made because the additional layers of patches will require further tuning to match impedance.

3.1.4 The Initial Design

Following on from the previous sections, the geometry and structure of the antenna are shown in table 3.1.

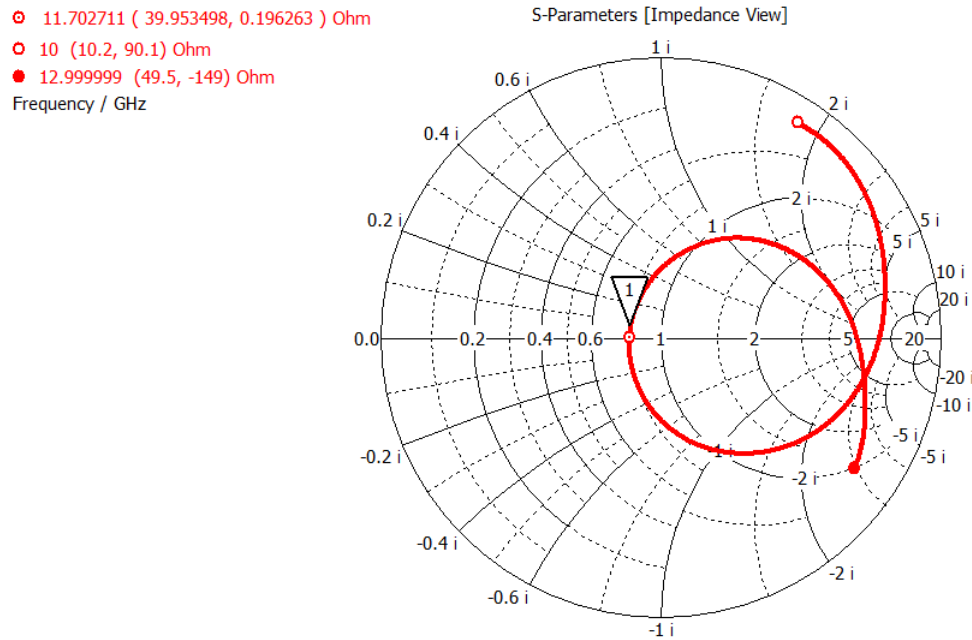


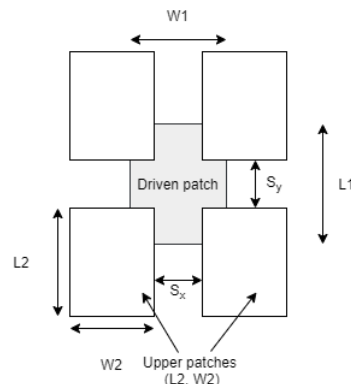
Figure 3.5 – The first layer Smith chart

Table 3.1 – Antenna dimensions.

Dimensions		
Part of antenna	Parameter	Value
First layer patch	Length	8.2mm
	Width	10.13mm
First layer substrate	ϵ_r	2.2
	Height	0.78mm

3.2 Second Layer Design

The second layer consists of four patches symmetrically located on the lower patch to overlap each corner. There is an important design consideration to remember and that is that the degree of coupling between the upper and lower patches is determined by the overlap area as well as the spacing between both layers. The height of the second layer is fixed at 1.58mm so controlling the coupling was done through the manipulating the overlap.



Design 22

Figure 3.6 – The first and second layer dimensions.

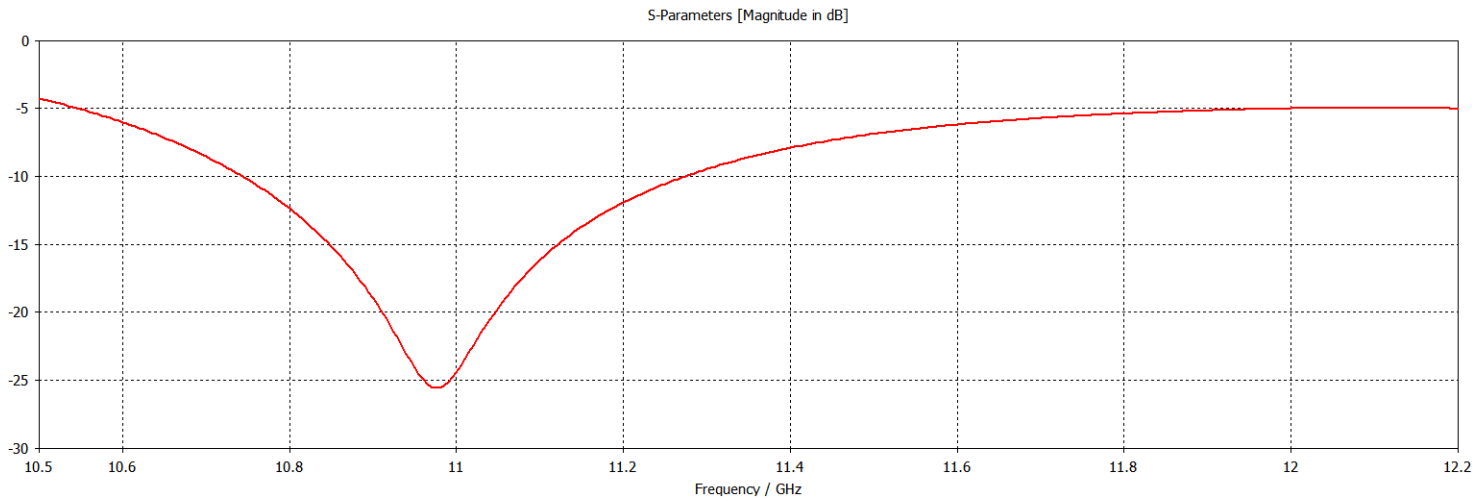


Figure 3.7 – S-parameters for the second layer simulation.

decreased. Firstly, the design equations 3.1-3.5 were used to calculate the dimensions with 11.95 GHz as the desired frequency. The newly calculated values were then entered into an parameter optimiser, this step ensured an efficient length was found without the need of an extensive parameter sweep. The optimised dimensions were all within 0.25mm of what was calculated and displayed in table 3.3.

Table 3.2 – Initial dimensions for second layer. **Table 3.3** – Optimised dimensions for second layer.

Dimensions	
Parameter	Measurement
L1	8.2 mm
W1	10.13 mm
L2	8.7 mm
W2	12.2 mm

Dimensions	
Parameter	Measurement
L1	7.3mm
W1	10.3mm
L2	8.2mm
W2	10.3mm

Table 3.4 – Second layer S-parameters and directivity with different spacing lengths.

Dimensions			
Parameter	Value	Return loss at 11.95 GHz	Directivity
$S_x = S_y$	3mm	-12.2dB	10.5dBi
$S_x = S_y$	2.3mm	-10dB	10.3dBi
$S_x = S_y$	1.6mm	-17.6dB	10.5dBi

Table 3.4 shows the best return loss and directivity results calculated with the optimised dimensions. Directivity for all spacing was passable, but only 1.6mm spacing provided an acceptable return loss at 11.95 GHz. Figure 3.8 shows -17.6dB return loss at 1.6mm

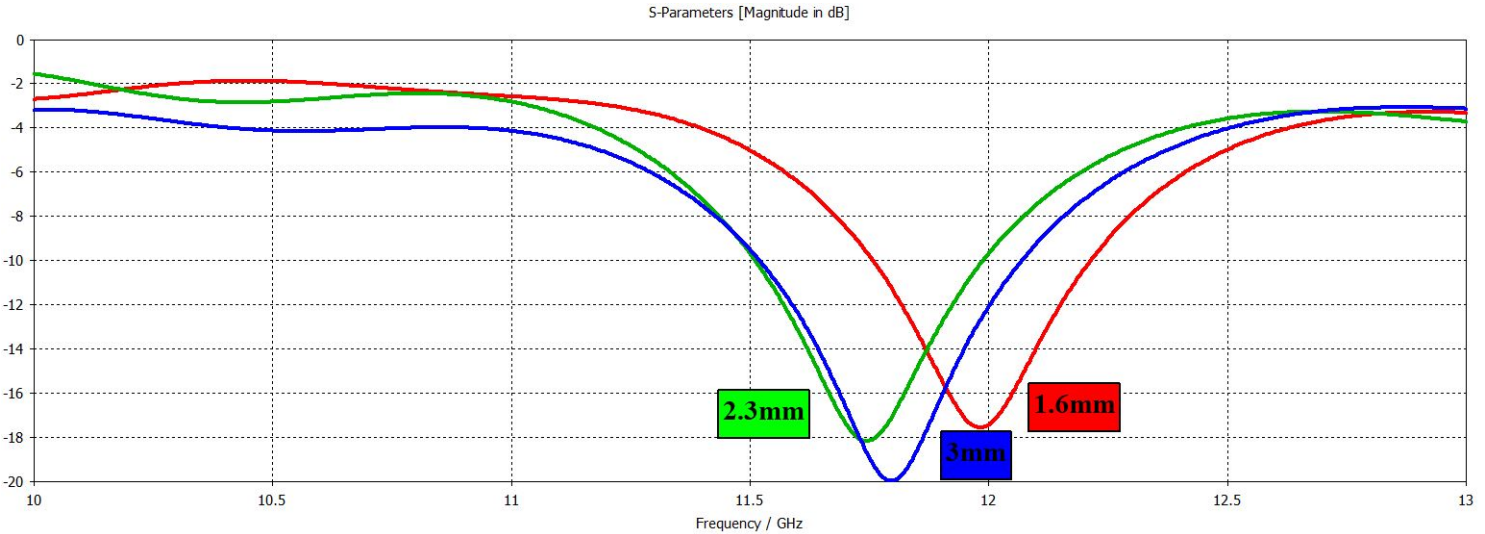


Figure 3.8 – Second layer S-parameters with spacing

spacing with a resonant frequency of 11.95 GHz and a -10dB bandwidth of 500 MHz. 1.6mm edge-to-edge separation is close to 0.1λ according to Balanis, this suggests small coupling along the H-plane with slightly larger coupling in the E-plane, the different coupling ratios were addressed by Legay and Shafai. In Legay and Shafai it was noted that in general, the transverse and longitudinal spacings are different when it comes to optimising antenna parameters and are used to eliminate imaginary impedance [16].

3.2.1 Planar Coupling

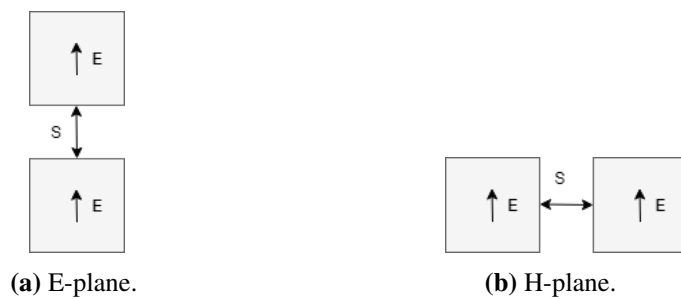


Figure 3.9 – E- and H- plane layouts of microstrip patch antennas.

For a rectangular microstrip, the propagation along the E-plane is TM and TE in the direction along the H-plane. For the E-plane configuration of Figure 3.9a, the elements are placed collinearly along the E-plane where fields in the area between the patches are primarily TM, there is substantial coupling because of the strong surface wave excitation. For the

H-plane configuration of Figure 3.9b, the fields between the elements are mostly TE and there is less coupling because there is no dominant mode surface wave excitation.

Figure 3.10 is an example of measured and calculated mutual coupling between two microstrip patches in the E and H planes with respect to spacing and wavelength [23]. The graph demonstrates how the E-plane has low coupling isolation for very small spacing while the H-plane exhibits low coupling isolation for large spacing.

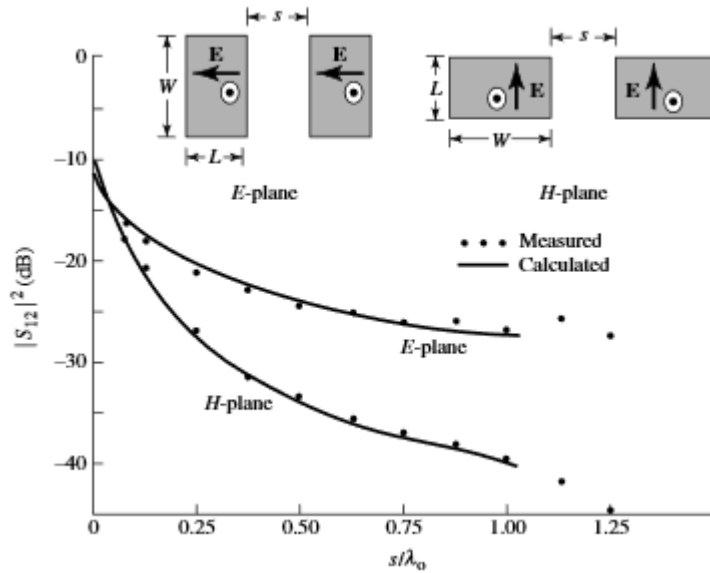


Figure 3.10 – Calculated and measured mutual coupling between two coax-fed microstrip antennas, for both E-plane and H-plane coupling ($W = 10.57\text{cm}$, $L = 6.55\text{cm}$, $h = 0.1588\text{ cm}$, $\epsilon_r = 2.55$, $f_r = 1.4\text{ GHz}$). (Source: D.M. Pozar, "Input Impedance and Mutual Coupling of Rectangular Microstrip Antennas," *IEEE Trans. Antenna Propagat.*, Vol. AP-30, No. 6, November 1982. ©1982 IEEE).

3.2.2 Second Layer Layout

Figure 3.11 shows the structure with the four patches of the second layer stacked onto the first.

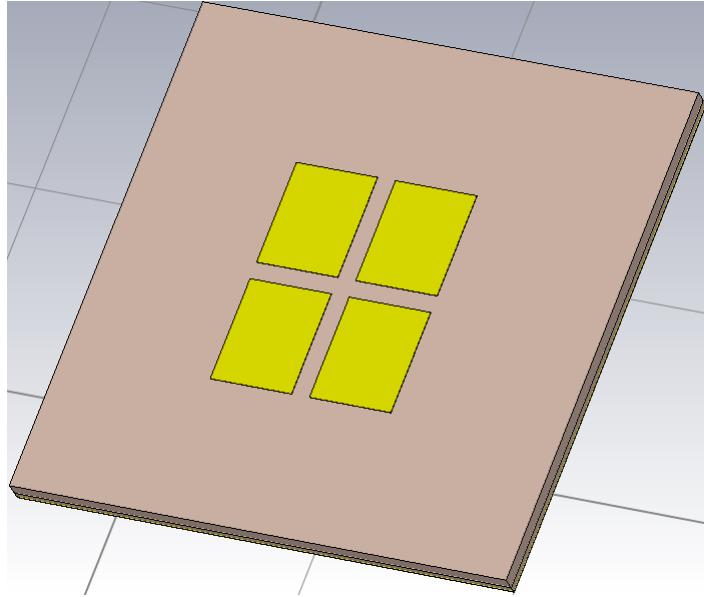


Figure 3.11 – The second and first layer model.

3.3 Third Layer Design

The third layer design takes after Nessel et al and aims to include an extra layer of patches to increase directivity and gain. The ROHACELL®31HF substrate height was set as close to 0.3λ as possible, that is 5mm. After the substrate height had been assigned, the patches on the third layer were placed symmetrically above the second. Initially the simulations did not produce expected results, especially in terms of S-parameters as shown below

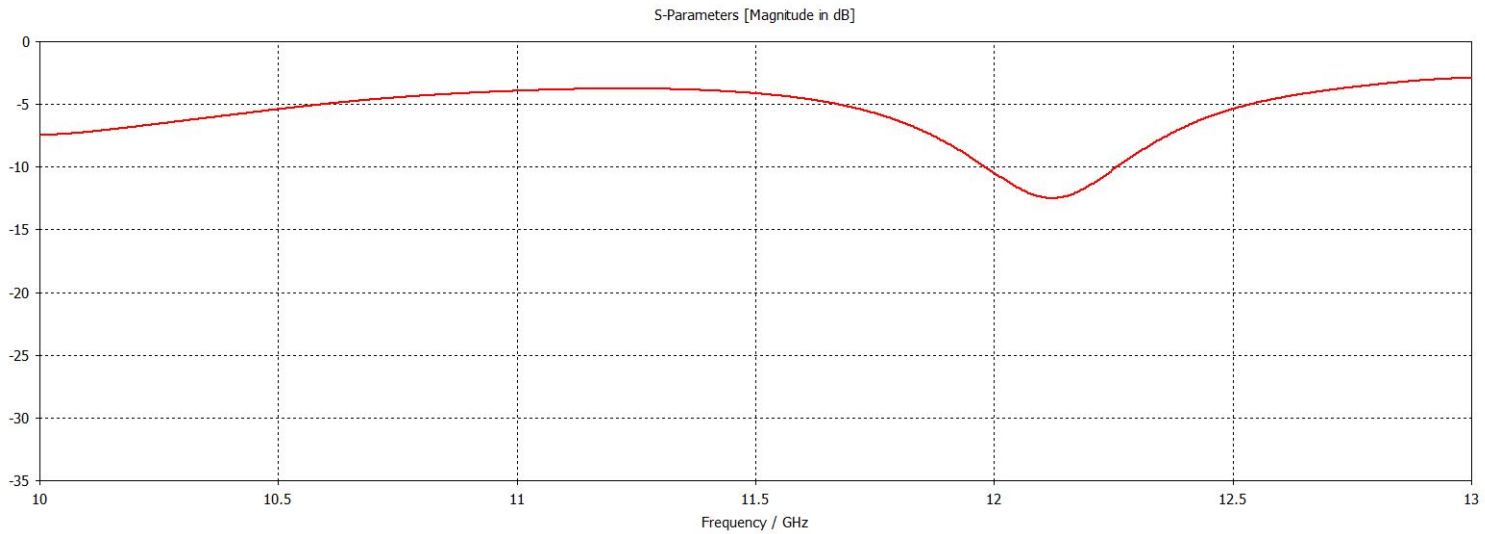


Figure 3.12 – First simulation for third layer where $h = 5\text{mm}$

There were multiple reasons as to why the S-parameters were not acceptable. Not only was the resonant frequency was too high, being close to 12.15 GHz, the return loss was below the minimum pass criteria of -15dB for the main lobe. The acceptable bandwidth was also too

narrow at just under 300 MHz. After inspecting the Smith chart in Figure 3.13, it was clear that the spacing between the second and third layer had to be manipulated due to the amount of real and imaginary impedance. In this configuration, the input impedance can be affected

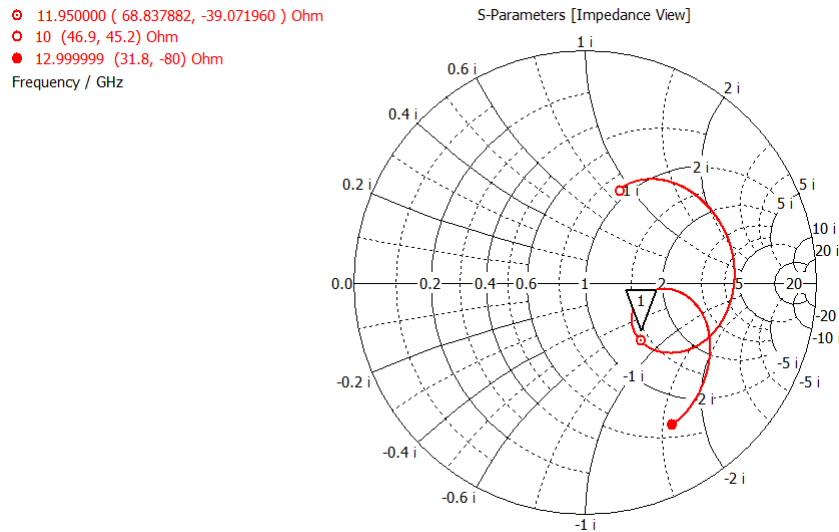


Figure 3.13 – Smith chart showing mismatched input impedance

by the level of coupling. Adjusting the spacing will help match the impedance but $50 + j0\Omega$ matching cannot be achieved without modifying upper and lower patch lengths. Changing the patch length means the amount of energy stored in the near field of the antenna can be reduced and the imaginary part of the impedance will decrease. Simulations also showed that adjusting the substrate height of the third layer altered the imaginary impedance, as seen below in Figure 3.14. This Smith chart above shows that a third layer thickness of 8mm has

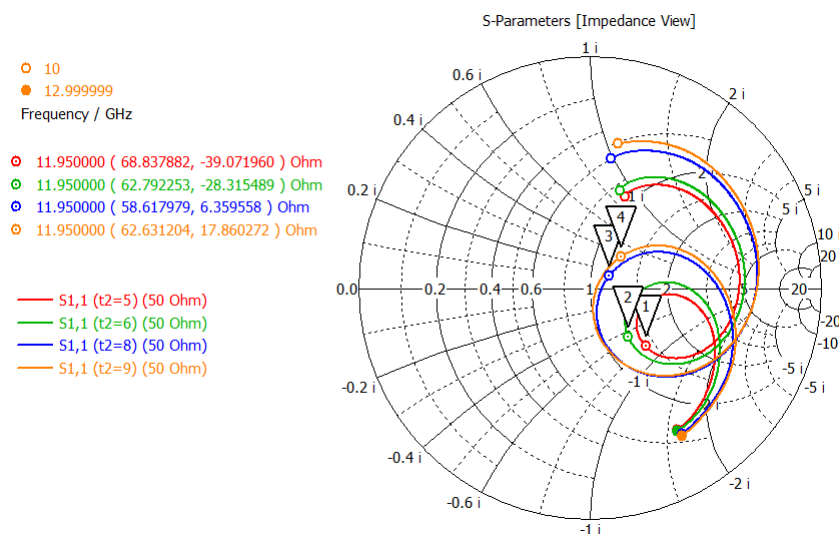


Figure 3.14 – Comparing Smith chart plots with respect to third layer substrate thickness.

an input impedance of $58.62 + j6.35\Omega$, that is 0.45λ , and is close to being critically coupled. With this result in mind, further adjustment of the patch dimensions could begin in an effort to achieve approximately $50 + j0\Omega$.

With all three layers attached the antenna height increased to 10.36mm, meeting the size and height requirement.

Dimensions	
Parameter	Measurement
L1	7.3mm
W1	10.3mm
L2	8.2mm
W2	10.3mm
L3	8.2mm
W3	10.3mm
First layer height	0.78mm
Second layer height	1.58mm
Third layer height	8mm

Table 3.5 – Patch dimensions after first acceptable simulation.

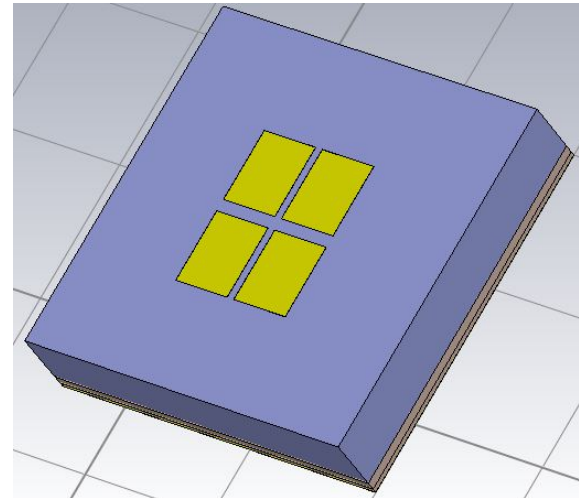
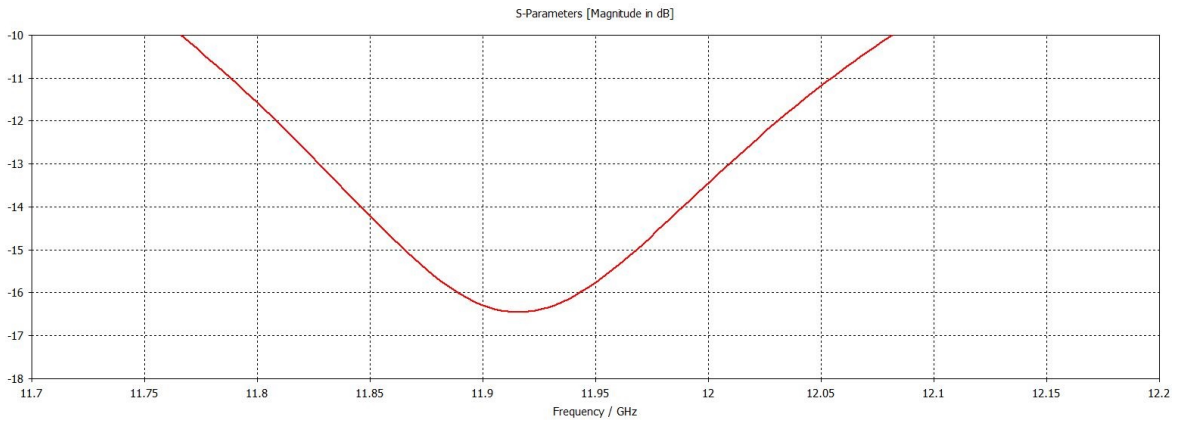
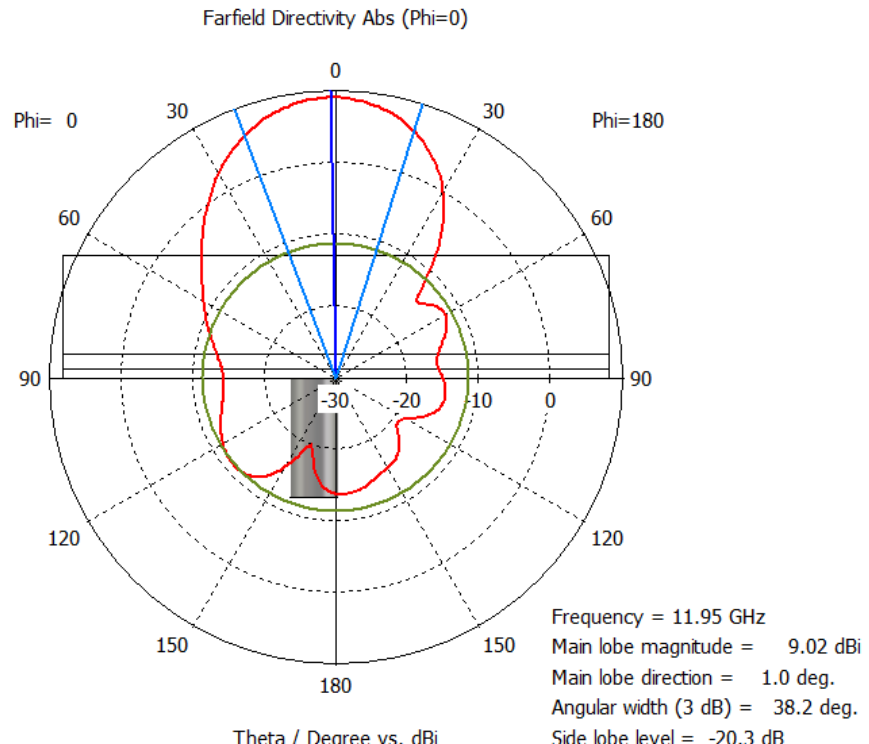


Figure 3.15 – The three layer stacked patch antenna with the foam height at 8mm.

The S-parameters with the dimensions of the table above were acceptable in terms of gain with a resonant frequency ≈ 11.95 GHz at -16.4dB. A bandwidth of 315 MHz was recorded, 185 MHz below what is needed, additionally, a directivity of 9.02dBi was measured. Both the directivity and bandwidth were lower than the two layer design and needed to be improved.



(a) S-parameters.



(b) Directivity.

Figure 3.16 – Directivity and S-Parameters for a third layer height of 8mm.

3.4 Antenna Tuning

The initial design was calculated using simple approximations, in order to improve the design simulation, full-wave methods in CST[®] were used to find more accurate measurements. Despite the input impedance almost matching 50Ω , unsatisfactory results were found due to the first layer being shorter, this went against the writings of Legay and Shafai, who stated the length of the lower patch must be longer than the upper patches [16]. Although the third layer would appear to be the root cause for the antenna's poor characteristics, there were other conditions that required modification.

3.4.1 Co-axial Probe

Before any patch or substrate dimensions were modified, the co-axial line impedance was inspected to make sure it was still 50Ω . Figure 3.17 shows an impedance of 50.37Ω at 11.95 GHz, this allows the antenna impedance to be matched to 50Ω .

Port1 e1	
Frequency:	11.95
Phase:	0
Line Imp. [Ohm]:	50.37

Figure 3.17 – Analytical line impedance of the co-axial probe.

3.4.2 Primary Changes To Element Spacing

Before any patch dimensions were changed, the overlap area from the second and third layers were altered in uniform. A parameter sweep from 3.2mm to 1.6mm for $S_x = S_y$ spacing was taken at 0.25mm intervals to measure the effect on antenna performance.

Moving the patches closer together increases the coupling area between the layer, however, after inspecting the Smith chart from Figure 3.14, the coupling for 8mm substrate thickness was close to critical, with $R = 58.6\Omega$. Although the edge-to-edge separation was close to ideal, it was not acceptable and the H-plane spacing was altered to $1.2\text{mm} \approx 0.07\lambda$.

3.4.3 Adjusting Substrate Height

After the H-plane alteration, a parameter sweep revealed that 5mm was not the optimal substrate height for the foam layer, instead 9mm showed promise with a gain of -60dB at the centre frequency.

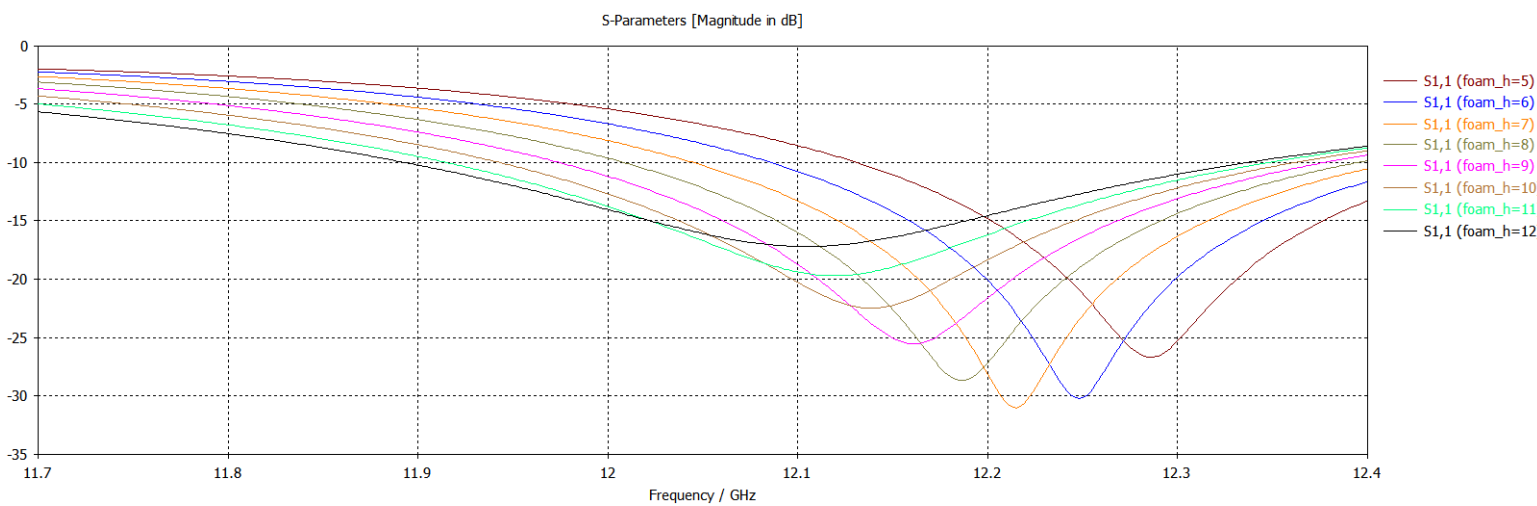


Figure 3.18 – Foam height parameter sweep from 5mm to 12mm.

3.4.4 First Layer Alteration

Although the S-parameters met the specification, gain and imaginary impedance still needed to be addressed. The first patch length was increased to 8.5mm to lower the centre frequency and allow the other patch layer lengths to be decreased. This technique was used to increase directivity and was inspired by the geometry of the Yagi-Uda-like antenna shown in Nessel et al, as a method of encouraging wave propagation in the direction of the directors [17].

3.4.5 Second and Third Layer Alteration

The lengths of the second and third layer patches were decreased to 7.2mm. Shortening the patches shifted the centre frequency higher and allowed for a greater overlap with 1.2mm spacing. This meant $S_X = S_Y = 1.2\text{mm}$. The final dimensions are displayed in the final chapter, see table 6.1.

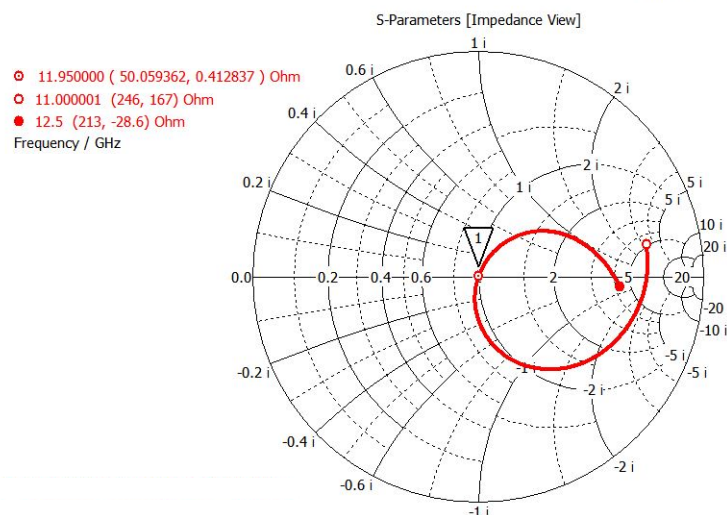


Figure 3.19 – Smith chart showing 50Ω impedance matching at 11.95 GHz.

The changes to the patch layers successfully matched the impedance to 50Ω , whilst improving bandwidth and directivity.

As the S-parameters suggest in Figure 3.20, the VSWR at the centre frequency is close to 1, with the side-bands reaching a maximum value of 2.3, see Figure 3.21. Finally, Figure 3.22 shows the final layout of the design.

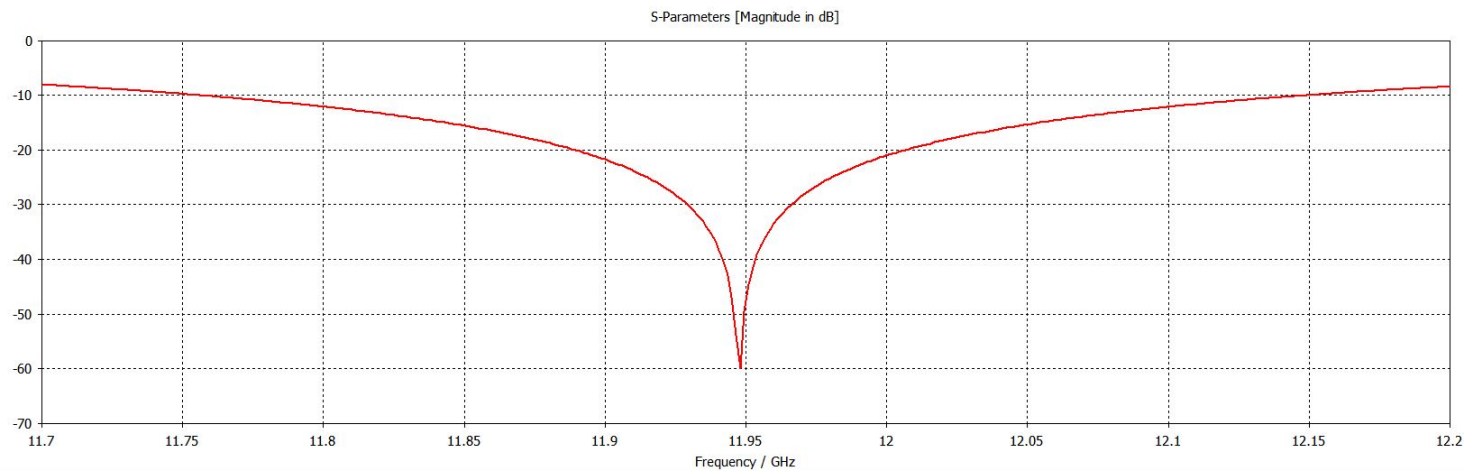


Figure 3.20 – The S-parameters for the final design.

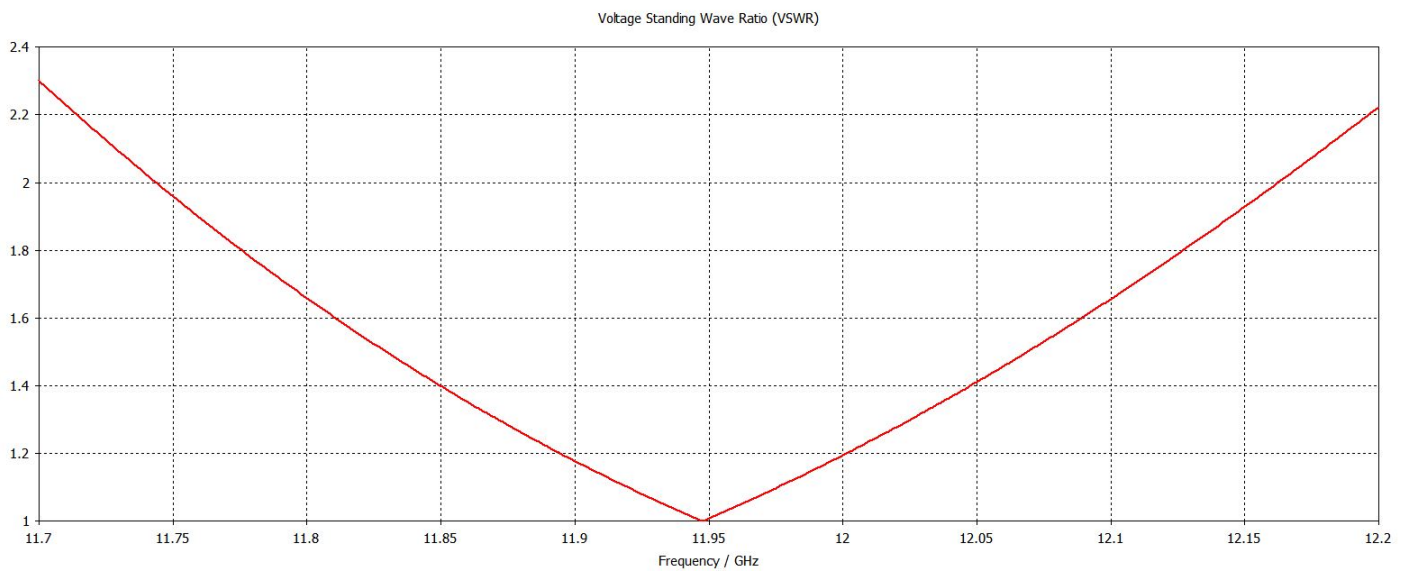


Figure 3.21 – VSWR for the final design.

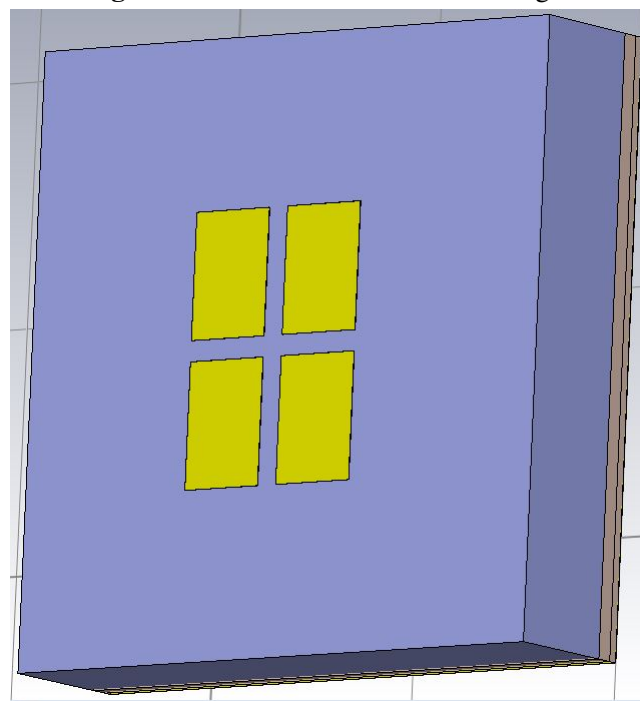


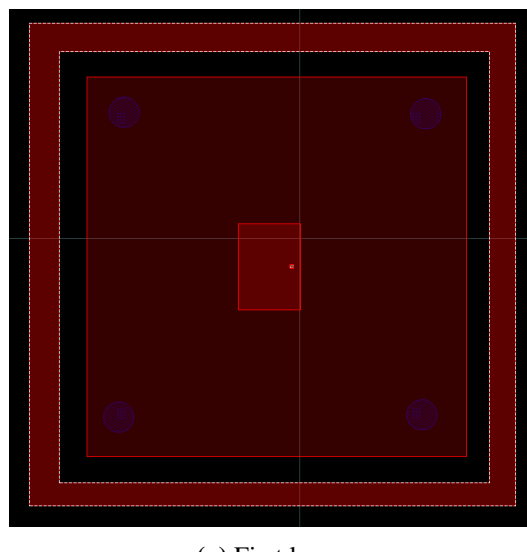
Figure 3.22 – The final design layout.

Chapter 4

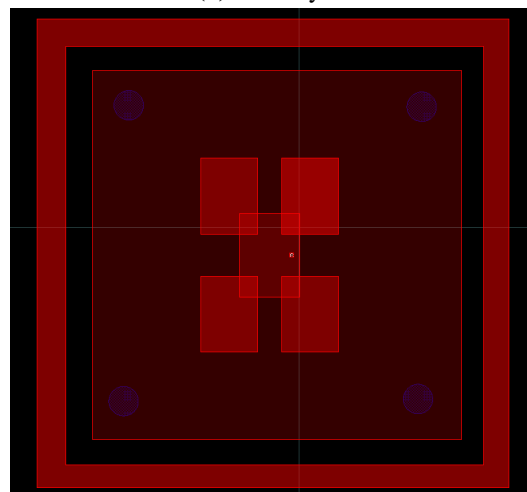
Fabrication

4.1 PCB Layout Design

ADS from Keysight Technologies was used to design the PCB layout and extract the Gerber and Drill files, see Figure 4.1. Only the first and second layers required design because the third layer is made of foam and copper adhesive tape.



(a) First layer.

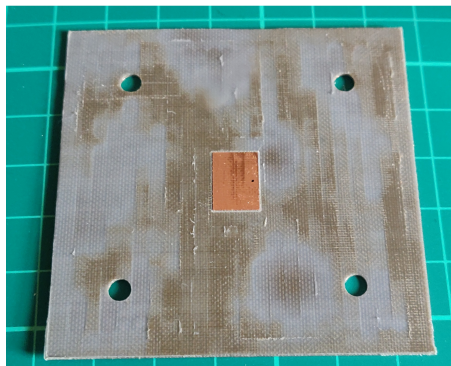


(b) All design layers.

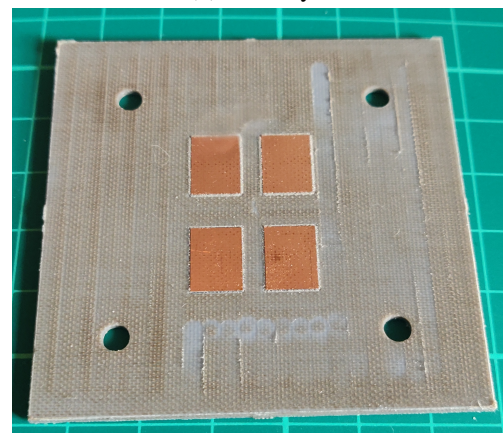
Figure 4.1 – First and second layers of the antenna on Duroid[®] 5880 substrate.

The designs were drilled and patterned with a PCB milling machine.

4.2 Antenna Construction



(a) First layer



(b) Second layer

Figure 4.2 – First and second layers of the antenna on Duroid[®] 5880 substrate.

Foam and copper tape made up the third layer, with nylons screws used to secure the layers together.

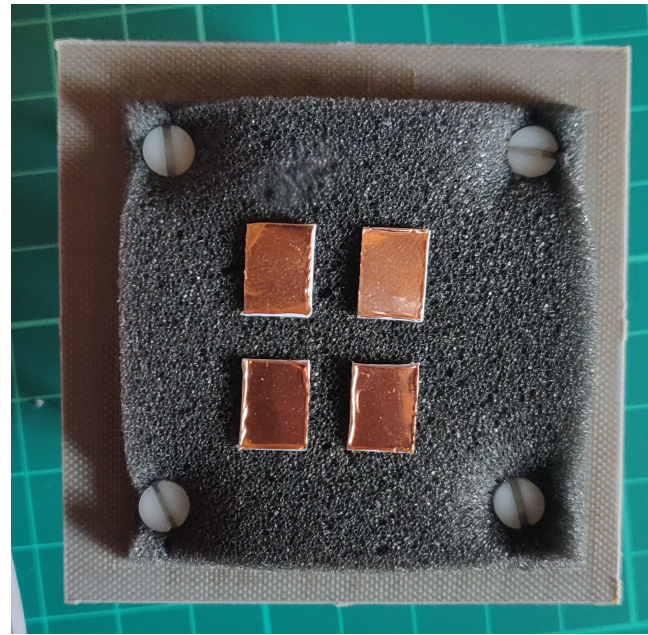


Figure 4.3 – Third layer fastened with nylon screws.

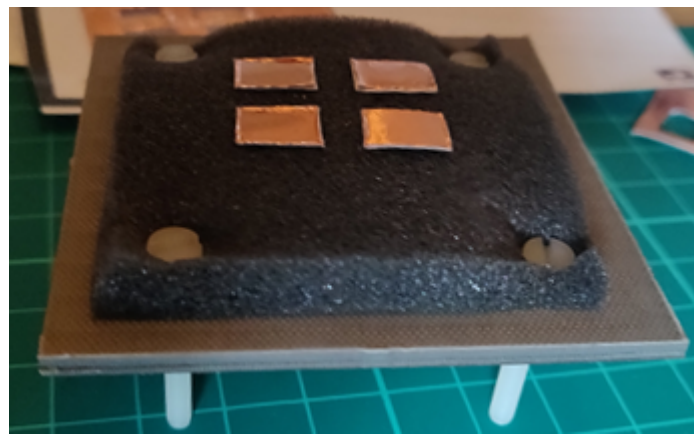


Figure 4.4 – Side view of the antenna.

Chapter 5

Project Planning

5.1 Agile Project Management

Since antenna development often involves revisiting design stages, agile management was chosen because of its iterative approach to product development. Agile development embraced iterations during the product life cycle phases which proved useful when tuning the antenna. There are two frameworks associated with agile, scrum and kanban. Kanban was used for this project because it focuses on identifying potential development bottlenecks.

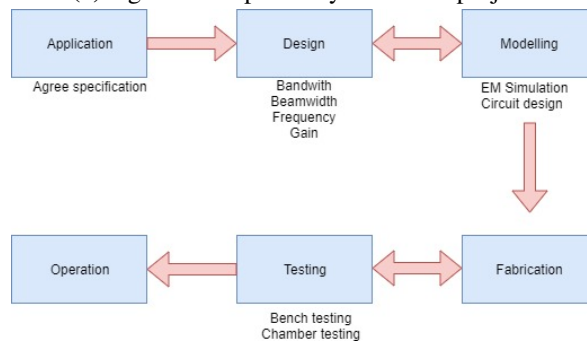
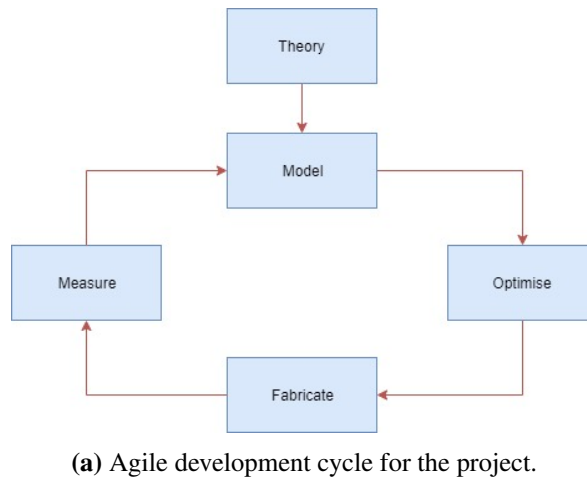


Figure 5.1 – Agile development block diagrams.

Once a specification was agreed the development entered the design stage where the antenna parameters were calculated, allowing the structure to be modelled. The double-sided

arrow indicates a sprint, a sprint is an approach in agile development that allows a large task to be broken down into small increments. Sprints allow agile planning to iterate over a certain design block until an acceptable product is created. The design and modelling stages were organised into small sprints because the two stages go back and forth until an acceptable simulation is produced. The same principle applies to fabrication and testing. Figure 5.1a outlines the core elements of the design cycle. Figure 5.1b follows the more traditional agile development plan.

5.2 Kanban

A kanban board is a project management tool that helps the user visualise workflow in order to maximise work efficiency. There are three core practices involved with kanban boards:

1. *Visualising the workflow.*

There are three columns in a kanban board, work selected for development, work in progress and work done. For example once item X has been selected for development it will stay in that column until it becomes a work in progress and once finished it is moved to the work done column, see Figure 5.2.

2. *Limit work in progress.*

Kanban boards are supposed to discourage multi-tasking as this can waste time. Setting a maximum number of items per stage ensure more focus and effort goes into the listed tasks.

3. *Managing workflow.*

A kanban board is implemented to create an efficient workflow. Workflow is defined as the movement of tasks through the kanban board.



Figure 5.2 – Kanban workflow.

5.3 Development Challenges

5.3.1 Maintaining Momentum

Agile development and Kanban ensured the project kept progressing through the use of sprints and regular feedback from a supervisor. The added advantage of having a supervisor is the ability to measure project performance and development rate through Kanban. Kanban allows

a supervisor to ensure the development is moving at an appropriate pace and not slowing down at any stage. A cumulative flow diagram provides a graphical representation of progress

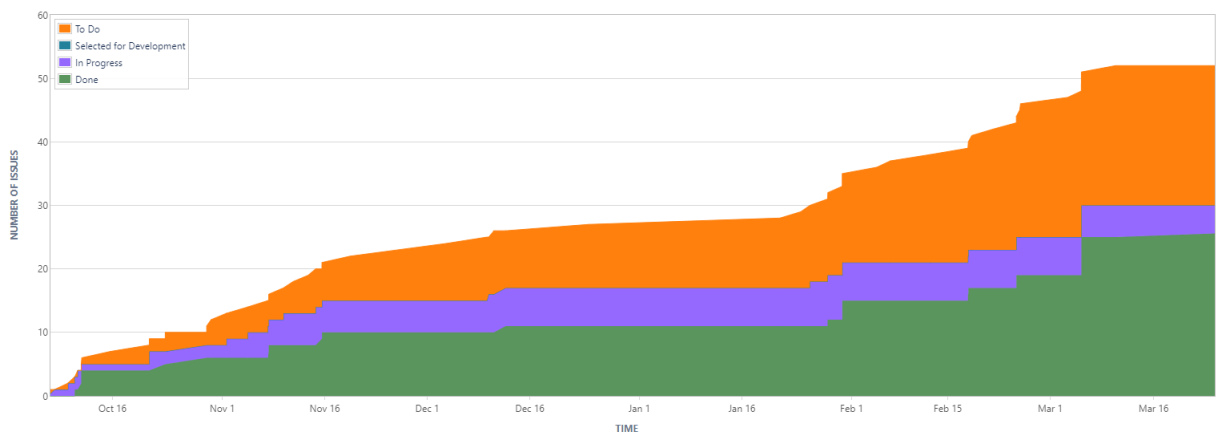


Figure 5.3 – Cumulative flow diagram from kanban board

and allowed for any disruptions to be discussed during meetings, see Figure 5.3.

5.3.2 Adapting To Change

Ensuring change is appropriately managed is an important feature of project planning because it ensures productivity continues through unforeseen circumstances. Some examples of change that have been identified during the product life cycle:

- *Misinterpreting design equations or theory*
- *Incorrectly calculating an equation*
- *Design requirements change*
- *Failed design approaches*

The entire product development cycle is a learning process and misinterpreting equations or theory is a part of this. Whenever a mistake was detected, it was noted and logged (Figure 5.4b) to avoid repetition. Confirmation from a supervisor was then sought to ensure the misunderstanding was gone. Given the flexible nature of agile development, mistakes are able to be corrected without impeding all stages. Once a mistake was identified it could be focused on and solved without affecting the entire design process.

During the early stages of the design, research was still being conducted on VSATs and the parameters required for the project. Frequent design changes in an engineering environment generally restrict progress and should ideally be avoided. However, this was not the case for this project because research was still being carried out during early phases of the

design so calculations were often repeated. To avoid doing more work than necessary, the research phase was finished before any further design work so time was not wasted.

Whilst testing numerous design variations found during research, not all designs provided the intended results thus failed to achieve the necessary criteria. Designs that did not go to plan were noted and logged so they were not repeated without intention.

5.3.3 Risk Management

For every risk involved with the project, it is important to have a contingency measure available so development may continue. Risk management is the process of categorising, identifying, prioritising and planning for risks. For this report, the definition of a risk is anything that could potentially impact the project timeline or performance. This was partly discussed in 5.3.2, this section will explain the risk identification procedure.

Risk identification involves creating a list of scenarios that will negatively impact product development. This stage contemplates what might happen and attempts to recognise why it happens. Once the risk has been noted, the likelihood and impact must be evaluated, this has been done. Some risks are more

Risks were logged into the kanban board, Figure 5.4a is an example of a risk being logged and Figure 5.4b shows where risks were positioned on the kanban board.

5.3.4 Project Planning Conclusion

Overall, the project planning was effective at producing results thanks to the clearly outlined workflow delivered through the kanban board. Having a clear development structure that could easily be visualised proved critical in ensuring a clear rate of development with minimal disruption was achieved. The board's built-in risk management feature made it easy to analyse, measure and mitigate risk allowing for near-optimal risk management.

During the project it was quickly discovered that all calculations should be carried out before running a simulation to avoid wasting development time. If too much time is spent running parameter sweeps or other simulations types, a lot of productivity diminishes, especially if the project is in the design block. It was learnt that time was a crucial factor throughout the entire project and simulations should be based on calculations or viable theoretical suspicion.

 CE301_yates_w / CE301P131-54

Incorrect impedance calculation

[Edit](#) [Comment](#) [Assign](#) [More](#) [Backlog](#) [Selected for Development](#) [Workflow](#)

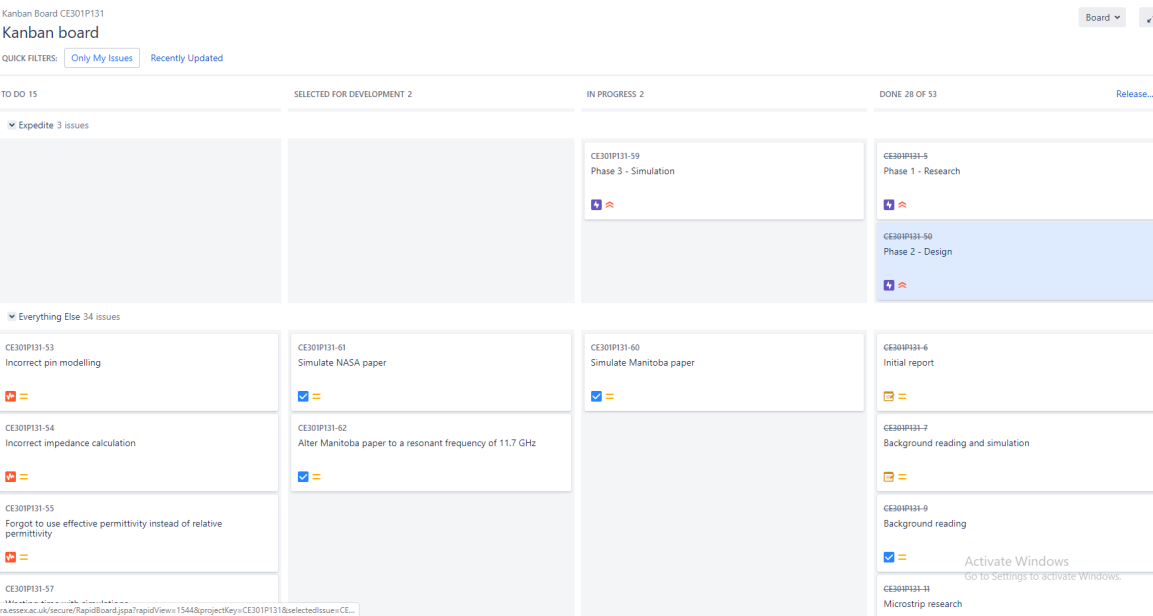
[Details](#)

Type:	Risk	Status:	BACKLOG (View Workflow)
Priority:	Medium	Resolution:	Unresolved
Labels:	None		

[Description](#)

There are two approximations used for calculating the edge impedance of a patch antenna. I must make sure to use the correct one at all times since the equations are based on the patch width and substrate thickness. These are volatile parameters so it is vital I ensure I use the correct approximation. An incorrect impedance may result in poor return loss.

(a) Example of a risk being issued to the kanban board.



(b) The kanban board during phase 3.

Figure 5.4 – This figure shows a risk being reported and the entire kanban board.

Agile development and the kanban framework worked very well for this project because it allowed sprints to be prioritised during the work in progress phase. Since kanban does not have a time boxed development cycle, sprints could be listed as the most important task without the pressure of a deadline. The only deadlines were project-related deliveries such as the an interim presentation or a poster day.

Chapter 6

Conclusions

6.1 Results

Figure 6.1 The centre frequency showed a directivity of 12.8dBi, with the lower sections of the bandwidth reaching up to 13.3 dBi. The directivity gain at 12.2 GHz was 12.3dBi, this means the antenna has met the criteria for directivity. The following results were recorded from the dimensions shown in the table below.

Dimensions	
Parameter	Measurement
L1	8.7mm
W1	10.3mm
L2	7.2mm
W2	10.3mm
L3	7.2mm
W3	10.3mm
First layer height	0.78mm
Second layer height	1.58mm
Third layer height	9mm
$S_x = S_y$	1.2mm

Table 6.1 – Table of the final antenna dimensions.

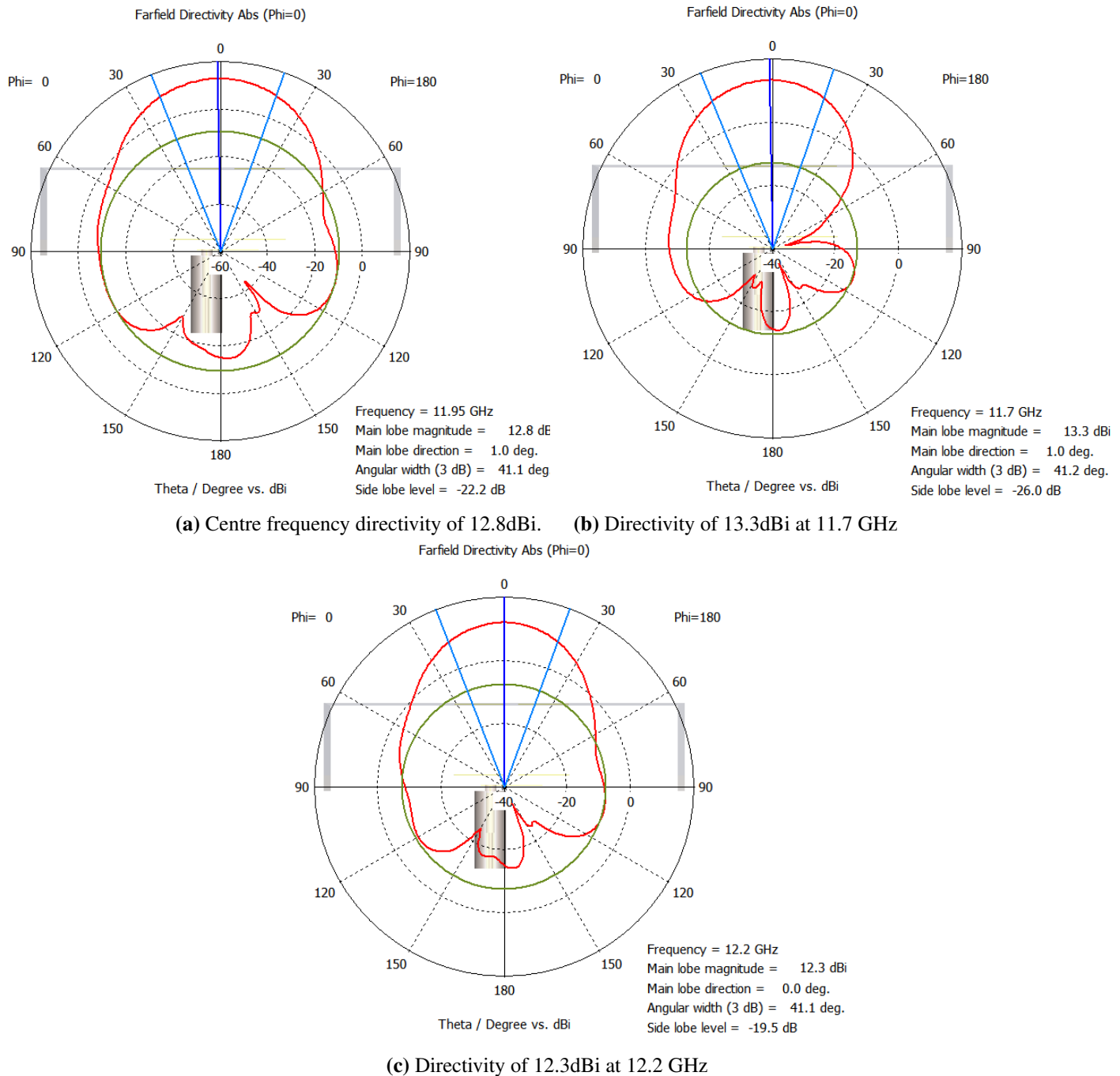


Figure 6.1 – Antenna directivity from 12.3 - 13.3dBi.

The antenna designed was able to pass the defined criteria, the main characteristics are displayed in table 6.2.

Final design parameters	
Parameter	Value
Resonant Frequency	11.95 GHz
Bandwidth	11.7-12.2 GHz
Beamwidth	31.7°
Directivity	12.3 - 13.3dBi
Dimensions	50mm x 50mm x 11.36mm
Weight	< 100g

Table 6.2 – Operating parameters for the final design.

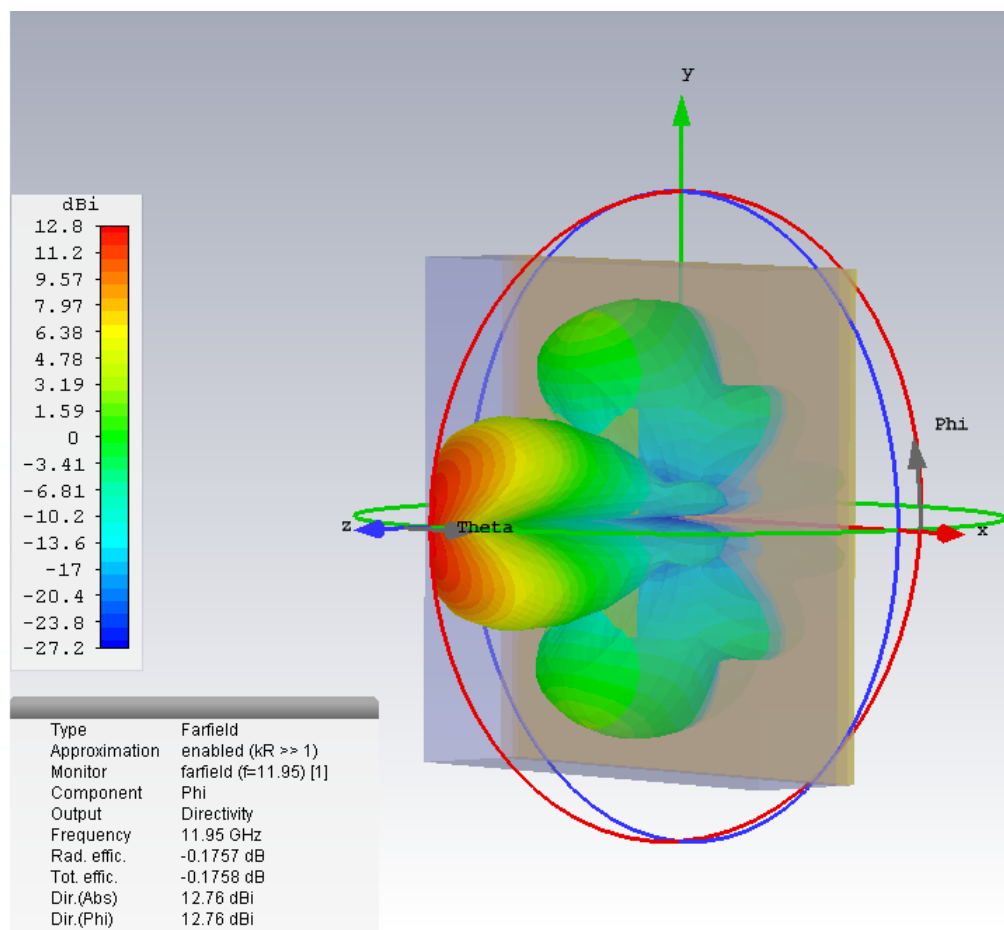


Figure 6.2 – E-phi radiation pattern at 11.95 GHz where phi = 0.

Figure 6.2 shows the centre frequency radiation for the E-field radiated with a radiation efficiency of $-0.1757\text{dB} \approx 96\%$.

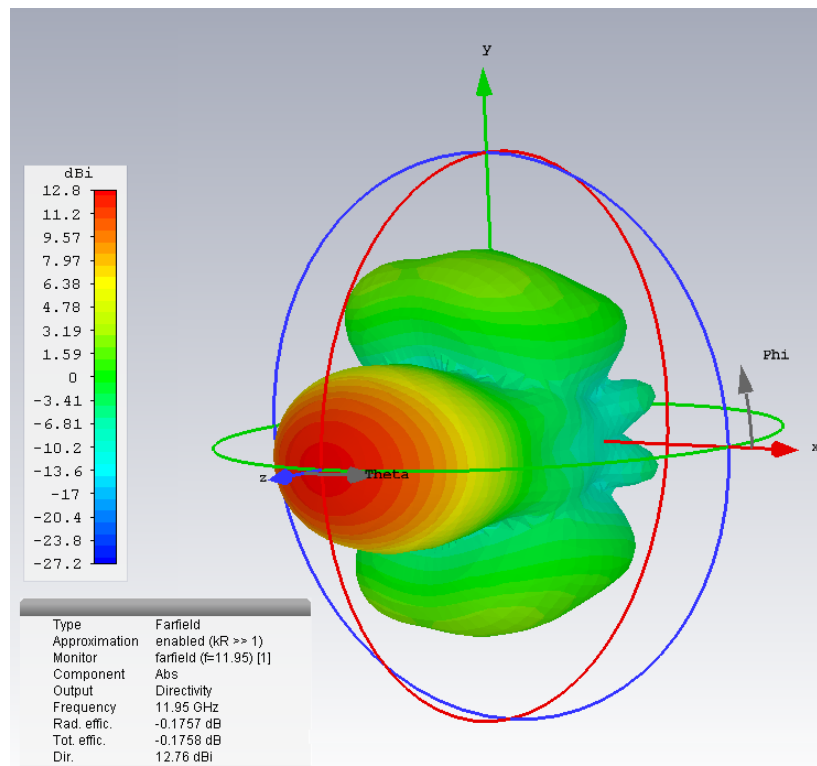


Figure 6.3 – Absolute radiation pattern at 11.95 GHz

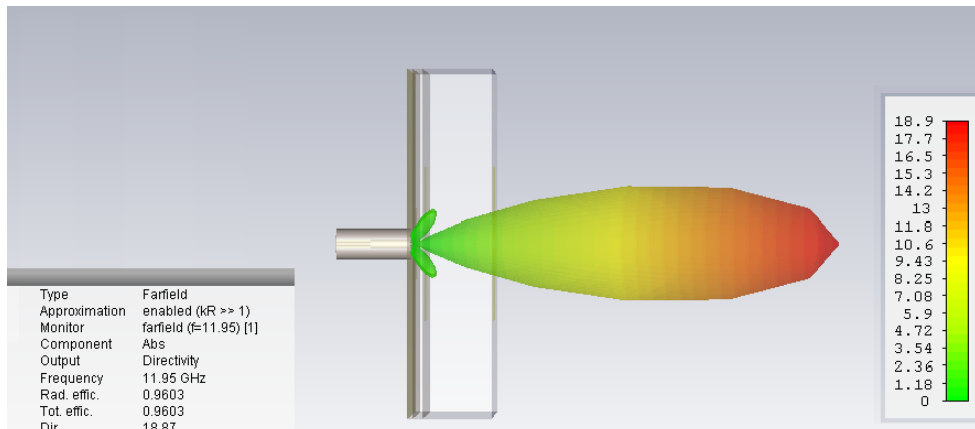


Figure 6.4 – Absolute linear directivity at 11.95 GHz

Figures 6.3 and 6.4 show the radiation patterns at 11.95 GHz, a logarithmic and linear comparison has been given to illustrate the strong directive property of the antenna.

6.2 Link Budget Example

Since the information carrying capacity of any radio communication link is determined by the RF power at the receiver input, the antenna designed will improve channel performance. A communication link is designed to meet a particular performance objective, in most cases this is a certain BER or SNR. This section shows how increasing the gain of a receive antenna can improve the CNR and BER of a communications channel.

The base-band BER or SNR is decided by the CNR at the input of a receiver [26].

The example link budget has a CNR of 15.37dB when the receive antenna gain was 7.5 dBi (average gain of a single patch), the CNR increased when the featured antenna was included in the analysis. With the stacked high-gain antenna in place, the CNR improved to 20.77dB. The improved CNR allows for higher order modulation schemes to be used because CNR is closely related to energy per bit to noise power spectral density ratio, that is

$$CNR = \frac{E_b}{N_0} f_b \quad (6.1)$$

$\frac{E_b}{N_0}$ is also known as normalised SNR and may be used to evaluate BER performance of different modulation schemes. BER as a function of SNR is shown in Figure 6.5 and shows that with a greater CNR, a lower BER is achieved and a more robust modulation scheme can be used [25].

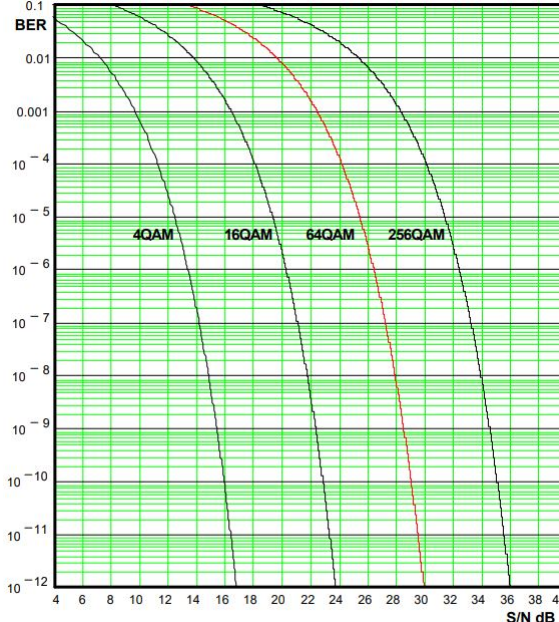


Figure 6.5 – BER as a function of SNR.

Ground station	
Parameter	Value
Uplink Frequency	14 GHz
Transmitter power	40dBW
Bandwidth	500 MHz
Antenna gain	41dBi
EIRP	81dBW
Uplink path loss	177dB
Uplink CNR	66.84dB/Hz

Table 6.3 – Ground station parameters.

VSAT	
Parameter	Value
Uplink Frequency	11.95 GHz
System noise temperature	75dB/K
Antenna gain	12.8dBi
Antenna G/T	-62.1dB/K
Downlink path loss	176dB
Downlink CNR	-46.07dB/Hz

Table 6.4 – Downlink station parameters.

Satellite		
Antenna gain	7.5dBi	12.8dBi
Satellite G/T	20.5dB/K	20.5dB/K
Satellite EIRP	50dBW	50dBW
Antenna G/T	-67.5dB/K	-62.1dB/K
Satellite PFD loss	-50.88dBW/m ²	-50.88 dBW/m ²
Overall CNR	15.37dB/Hz	20.77dB/Hz

Table 6.5 – CNR comparison for 7.5dBi and 12.8dBi receiver antennas.

The tables above show the overall link budget, table 6.5 compares the CNR with a 7.5dBi antenna and the designed antenna. Overall CNR improved with the designed antenna and therefore a strong communications link could be established.

6.3 Project conclusion

Overall, the project was a success as it met the criteria specified in the technical documentation. The final simulation produced the intended results, allowing an antenna to be built from the design which could satisfy the design requirements

- *Resonant frequency.* With a resonant frequency of 11.95 GHz at -60dB, the antenna has met the sought after centre frequency with a low reflection loss.
- *Bandwidth.* A 500 MHz bandwidth was observed, this is enough to support a high-capacity communications link such as satellite broadband.
- *Directivity* With directivity over 12dBi, the antenna is able to concentrate 93.7% of its radiated power in a certain direction, allowing the device to be directed towards a satellite constellation.
- *Dimensions* The antenna produced is smaller than a parabolic antenna with a 0.7m diameter as intended.
- *Weight.* The antenna weights less than 100 grams as specified.

Future work on the design may include additional director layers to increase directivity, however, there is a limit to the number of feasible layers needed before they are redundant or the design becomes too tall to meet the specification. The gain increase per layer falls by approximately 0.5dB each stack, this means that each layer becomes increasingly redundant.

The third layer was the most difficult to construct because it involved cutting four equally-sized rectangles and laying them in a precise configuration on a small piece of foam. This made it very difficult to produce the patches to the desired measurements and find the correct placement. It was evident that this stage of the fabrication needed improvement.

A thin layer of Duroid[®]5880 with a thickness of 0.127mm would allow for the top layer design to be chemically etched onto it. 0.127mm of substrate is thin enough not to adversely affect the S-parameters or directivity of the antenna. A benefit of chemical etching over manually constructing the patches is the patch dimension and arrangement accuracy. The design may be printed onto the substrate, which has the advantage of machine precision. With the size of the patches, chemical etching is a more accurate and reliable method than construction by hand.

Bibliography

- [1] C.A. Balanis. *Antenna Theory, Analysis and Design*, 4th ed. Hoboken: John Wiley Sons, 2016.
- [2] T. Pratt, C. Bostian and J. Allnutt. *Satellite Communications*, 2nd ed. New Jersey: John Wiley Sons, 2003.
- [3] J.L. Volakis. *Antenna Engineering Handbook*, 5th ed. New York: McGraw-Hill, 2019.
- [4] J.Howell. "Microstrip antennas", in *1972 Antennas and Propagation Society International Symposium*, volume 10, pp.177-180.
- [5] Rogers Corporation, "High Frequency Laminates", RT/duroid 5870/5880 datasheet, 2010 [Revised 2017].
- [6] Ofcom. *The Future of Fixed Telephone Services: Policy Positioning Statement*, Feb 22, 2019. [Online].
Available: https://www.ofcom.org.uk/__data/assets/pdf_file/0032/137966/future-fixed-telephone-services.pdf
- [7] D. Bogdan-Martin. *Measuring Digital Development : Facts and Figures*, International Telecommunication Union., Geneva, 2019.
- [8] A. Sharma. *ITU Calls to Connect Almost 4 Billion Unconnected Individuals Globally*, The National(UAE). Oct 28, 2018. Accessed: Apr 2, 2020. [Online]. Available: <https://www.thenational.ae/>
- [9] S. Badombena-Wanta and E.O Sheybani, "Mobile communications for development: Enabling strategic and low-cost e-applications for rural and remote areas," in *Proc. Wireless Telecommun. Symp. (WTS)*, Tampa, FL, USA, Apr. 2010, pp. 1-7.
- [10] A. Sey, C. Coward, F. Bar, G. Sciadas, C. Rothschild and L. Koepke. *"Connecting*

People for Development: Why Public Access ICTs Matter", Univ. Washington., Seattle, Washington, 2013.

- [11] S. S. Chakravarthy, N. Sarveshwaran, S. Sriharini and M. Shanmugapriya, "Comparative study on different feeding techniques of rectangular patch antenna," 2016 Thirteenth International Conference on Wireless and Optical Communications Networks (WOCN), Hyderabad, 2016, pp. 1-6.
- [12] A. Kumar, J. Kaur and R. Singh, "Performance Analysis of Different Feeding Techniques," *International Journal of Emerging Technology and Advanced Engineering*, vol.3, pp.884-889, Mar 2013.
- [13] William A. Imbriale; Steven (Shichang) Gao; Luigi Boccia, "Antenna Basics," in *Space Antenna Handbook* , Wiley, 2012, pp.1-35
- [14] K. Lee and K. Tong, "Microstrip Patch Antennas—Basic Characteristics and Some Recent Advances," in *Proceedings of the IEEE*, vol. 100, no. 7, pp. 2169-2180, July 2012.
- [15] F. E. Gardiol and J. Zurcher, "Broadband patch antennas-a SSFIP update," *IEEE Antennas and Propagation Society International Symposium*. 1996 Digest, Baltimore, MD, USA, 1996, pp. 2-5 vol.1.
- [16] H. Legay and L. Shafai, "A new stacked microstrip antenna with large bandwidth and high gain," *Proceedings of IEEE Antennas and Propagation Society International Symposium*, Ann Arbor, MI, USA, 1993, pp. 948-951 vol.2.
- [17] J. A. Nessel, A. Zaman, R. Q. Lee and K. Lambert, "Demonstration of a X-band multilayer Yagi-like microstrip patch antenna with high directivity and large bandwidth," *2005 IEEE Antennas and Propagation Society International Symposium*, Washington, DC, 2005, pp. 227-230 vol. 1B.
- [18] J. L. Volakis. "Wideband Microstrip Antennas" in *Antenna Engineering Handbook*, 4th edition, New York: McGraw Hill, 2007, pp. 16-17.
- [19] I. J. Bahl and P. Bhartia, *Microstrip Antennas*, Artech House, Dedham, MA, 1980.

- [20] Cinch Connectivity Solutions, "142-1701-201 Product Information", 50 Ohm SMA 2-Hole Flange Mount Jack Receptacle - Extended Dielectric. [Revised 2017].
- [21] D. M. Pozar,"A Review of Aperture Coupled Microstrip Antennas: History, Operation, Development, and Applications," 1996. Available: <http://www.eecs.umass.edu/ece/pozar/aperture.pdf>.
- [22] L.Shafai, P. Mousavi and R. Mrizavand, "Wideband Microstrip Antennas", in *Antenna Engineering Handbook*, J. L. Volakis. 5th edition, New York: McGraw Hill, 2019, pp. 216.
- [23] D. M. Pozar, "Input Impedance and Mutual Coupling of Rectangular Microstrip Antennas," *IEEE Trans. Antenna Propagat.*, Vol. AP-30, No. 6, November 1982. ©1982 IEEE.
- [24] W. O. R. D. Yates, "Design of a Ku-band High-Gain Corner-Coupled Planar Antenna For Low Earth Orbit Satellite Communications", (2020), GitLab repository. Available: https://cseegit.essex.ac.uk/ce301_2019/ce301_yates_w
- [25] Rohde Schwarz, "Bit Error Ratio BER in DVB as a Function of S/N", May 2002. Available: https://cdn.rohde-schwarz.com/pws/dl_downloads/dl_application/application_notes/7bm03/7BM03_4E.pdf
- [26] T. Pratt, C. Bostian and J. Allnutt. *Satellite Communications*, 2nd ed. New Jersey: John Wiley Sons, 2003, pp. 100-101.
- [27] D. R. Jackson and N. G. Alexopoulos, "Simple approximate formulas for input resistance, bandwidth and efficiency of a resonant rectangular patch," *IEEE Transactions on Antennas and Propagation*, vol. 39, no. 3, pp. 407–410, 1991.
- [28] Shannon, C.E. "A mathematical theory of communication," *Bell Syst. Tech. J.* 1948, 27, 379–423, 623–656. Reprinted in C.E. Shannon and W. Weaver *The Mathematical Theory of Communication*; University Illinois Press: Champaign, IL, USA, 1949.
- [29] D. Roddy. *Satellite Communications*, 4th ed. New York: McGraw-Hill, 2006, pp. 159-

- [30] Wikipedia contributors. "Microstrip antenna", Wikipedia.com, 2020,[Online]. Available: https://en.wikipedia.org/wiki/Microstrip_antenna [Accessed: April 5, 2020].
- [31] J. Bevelacqua. "The Parabolic Reflector Antenna (Satellite Dish)", *antenna-theory.com*, 2011. [Online]. Available <http://www.antenna-theory.com/antennas/reflectors/dish.php>. [Accessed Apr. 5, 2020.]